UNITED NATIONS UNIVERSITY
GEOTHERMAL TRAINING PROGRAMME
Orkustofnun, Grensasvegur 9,
IS-108 Reykjavik, Iceland

Reports 2012
Number 22

HYDROLOGICAL FLOW AND THERMAL INTERFERENCE MODELLING IN THE MAHANAGDONG GEOTHERMAL FIELD, PHILIPPINES, USING FOUR TYPES OF NAPHTHALENE DISULFONATE TRACER

Gary C. Mondejar
Resource Management Division, Technical Services Sector
Energy Development Corporation – EDC
38/F One Corporate Centre, Julia Vargas corner Meralco Avenue
Ortigas Center, Pasig City 1605
PHILIPPINES
gary.mondejar@gmail.com

ABSTRACT

The Mahanagdong geothermal field has been supplying steam since 1997 to its two power plants with a total installed capacity of 180 MWe. The field employs 100% brine reinjection and tracer testing has been used as one of the main tools in optimizing the reinjection strategy. A tracer test using four types of naphthalene disulfonate tracer was conducted in June 2011. Three tracer types were injected into three reinjection wells in the northern injection sink to evaluate the effects of brine returns, while a fourth type of tracer was injected into MG-4DA, a well located in the western part of the field, shut throughout the tracer test duration, to trace the inflow of groundwater to the production sector. More than 900 samples were collected within a year of monitoring. Tracer test results indicate that under the conditions during the tracer monitoring, reinjection in the northern injection sink did not cause a significant return of reinjected brine as to have any significant effect on the production sector. However, tracer analysis results for groundwater downflow through well MG-4DA yielded disquieting results. Thermal interference modelling indicated that for the pessimistic scenario of a 10 kg/s downflow rate in well MG-4DA, a maximum temperature decline of 1.4°C was predicted after 20 years. The predicted decline in temperature of the well affected by groundwater inflow was then compared with the actual cooling observed. Data on measured cooling from 2003 to date indicated that actual temperature decline of all the affected wells was higher than the predicted temperature decline, even after 20 years. This finding suggested that an even greater inflow of groundwater – greater than the downflow observed in well MG-4DA – exists and must, therefore, be estimated. Groundwater inflow modelling was conducted and results indicated that the rate of groundwater inflow to the production sector is estimated to be around 200 – 300 kg/s. Calculation of the average groundwater velocity indicated that the downflow observed in well MG-4DA could most likely be just a small part of a much greater groundwater inflow towards the production sector. Management interventions with regard to reinjection strategies, pre-emptive groundwater encroachment, long-term field development, as well as developing a more detailed 3D numerical model are presented.

1. INTRODUCTION

Stringent environmental laws in the Philippines mandate geothermal fields in the country achieve zero disposal of effluent. It is, therefore, imperative to reinject extracted geothermal fluids – separated brine and power plant condensates – back into the reservoir (Angcoy et al., 2008). Reinjection has been an efficient method of disposing of waste water, as well as a means of providing additional recharge to geothermal systems. With the continuous commercial exploitation of geothermal fields, the additional recharge that reinjection provides counteracts reservoir pressure drawdown. It also enhances the process of thermal extraction from reservoir rocks along flow-paths from reinjection wells. However, reinjection poses the possible danger of cooling production wells as the reinjected fluids travel back to the production area (Axelsson, 2012). Thus, monitoring reinjection returns and formulating an optimum reinjection strategy is a must in order to sustain the generation capacity of geothermal fields.

The detrimental cooling effect of reinjected fluids can be evaluated and managed through tracer tests. Tracer testing has been one of the main tools in optimizing the reinjection strategy of Mahanagdong geothermal field as it provides information on the hydrological connections between reinjection and production wells, and enables a quantitative assessment of cooling effects due to long-term reinjection. The first Mahanagdong tracer test was conducted in 1994, prior to commercial operation of the geothermal field which commenced in 1997. Sodium fluorescein was used to test whether utilization of a candidate reinjection well would interfere with the nearby production wells. The second tracer test, which also used sodium fluorescein, was conducted in April 1999, about two years after the start of commercial exploitation. This tracer test was conducted to evaluate the effects of utilizing a reinjection well on the nearby production wells. Also, in October 1999, another tracer test was conducted using a radioactive ^{125}I tracer solution. The objective of the ^{125}I tracer test was to study and quantify the extent of cold groundwater influx in the western part of the field which was found to have deleterious effect on the steam supply (Delfin et al., 2001). In 2003, three different types of naphthalene disulfonate (NDS) tracer were injected into three wells to determine the hydrological flow of cooler peripheral fluids to the production sector. Injection of tracer into one well was meant to evaluate the flow of natural groundwater recharge in the western part of the field, while tracer injection into the other two wells aimed at evaluating the flow of reinjected brine in the field's northwest and southeast section, respectively (Herras et al., 2005).

Since the 2003 NDS tracer test, eleven more production wells have been drilled, with the latest well completed in September 2011. Consequently, continuous field exploitation further aggravated the reservoir pressure drawdown. The latest reservoir assessment update by Mondejar et al. (2011) indicated that the field's highest drawdown of about 4.5 MPa was in the central production area where most of the production wells are concentrated. Hence, since the 2003 tracer test, changes in the hydrological flow of cooler fluids towards the production sector are to be expected.

This paper will present and discuss the results of the latest tracer test conducted in Mahanagdong last June 2011. The tracer test is meant to update the extent of the observed cooler fluid inflow, and map out whether the wells drilled after the 2003 tracer test are also affected by these cooler fluids. To achieve this objective, four different types of NDS tracer were injected. Three of these tracers were injected into three wells in the northern reinjection area of the field to evaluate the flow of brine returns, while the fourth tracer was injected into a well located in the western part to evaluate the inflow of natural groundwater. This natural groundwater inflow will be modelled to estimate its flow rate towards the production sector. This paper will also model and quantify the expected degree of cooling in the affected production wells. Lastly, it will present recommendations to further optimize the current reinjection strategy to better manage the reservoir.

2. MAHANAGDONG GEOTHERMAL FIELD

The Mahanagdong geothermal field, herein referred to as Mahanagdong, is a high-temperature geothermal system located on the island of Leyte in the central part of the Philippines (Figure 1). It lies within a large reserve area known as the Greater Tongonan geothermal field (GTGF), which is comprised of two geothermal fields – the Tongonan geothermal field in the north, and the Mahanagdong geothermal field in the south. These two fields are believed to be two distinct geothermal systems separated by a cold and impermeable barrier.

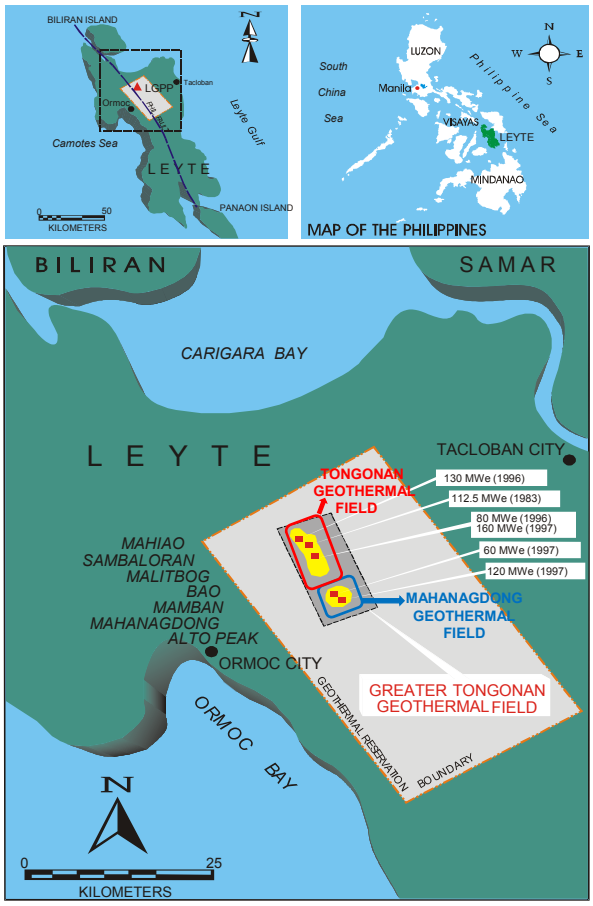

FIGURE 1: Mahanagdong geothermal field on the island of Leyte, Philippines

Recent integrated resource boundary estimates for Mahanagdong by Olivar (2011) indicated that the field has a minimum areal extent of 10.4 km^2 and a maximum of 14.5 km^2, although portions of the boundary, particularly to the northeast, are still highly speculative. The field is divided into two sectors: Mahanagdong-A which has a 2×60 MWe main plant and a 2×6.4 MWe optimization plant, and a 60 MWe Mahanagdong-B with a 6.4 MWe optimization plant.

Commercial exploitation of Mahanagdong commenced in July 1997 with more than 270 kg/s of steam available for Mahanagdong-A, more than enough to supply the main plant. Mahanagdong-B had more than 130 kg/s of steam available, also enough to meet the full-load requirement (Herras et al., 2005). However, since June 1998, Mahanagdong has been having difficulty meeting the full-load requirement of 180 MWe. Processes that contributed to steam decline in the field, as well as the strategies implemented to address the steam shortfall, will be discussed in later sections.

2.1 Geological overview

The island of Leyte is traversed by the NW-SE trending Philippine Fault which is a major sinistral fault that runs through the whole length of the Philippine archipelago. The complex fault network associated with the Philippine Fault system generally provides the fluid flow channels in GTGF (Caranto and Jara, 2006).

The stratigraphy of Mahanagdong is composed mainly of five major lithologic units, namely: Bao volcanics, Mamban formation, Mahanagdong claystone, Mahiao sedimentary complex, and the basement complex. The youngest among these formations is the Bao volcanics, Pliocene to Pleistocene in age, composed mainly of andesite lavas intercalated with vitric tuffs. The oldest rock unit is the Pre-Tertiary Basement Complex which consists of serpentinized peridotites, diorites, and metamorphics (Austria and Villareal, 2012).

Most of the wells in Mahanagdong have their production casing shoes set within the Mamban formation, which is composed of moderate to intensely altered biotite-bearing andesite and tuff breccias

interbedded with calcareous sandstone and carbonaceous siltstone. On the other hand, the formation where most of the wells are bottomed is within the Mahiao sedimentary complex, which is composed of sedimentary breccias with intrusive clasts, tuffs, hornfels, andesite, argillized and silicified fragments set in an argillaceous matrix (Pioquinto, 2011).

2.2 Conceptual model

Mahanagdong has a distinct upwelling region separate from that of the Tongonan geothermal field. A baseline conceptual model (1997) suggested that the upflow surges vertically in the region around wells MG-3D and MG-14D, where downhole temperatures of more than 310°C exist at depths (Figure 2). Upwelling fluids laterally outflow to the south at well MG-5RD and to the southwest in the area around well MG-1 (Sta. Ana et al., 2002).

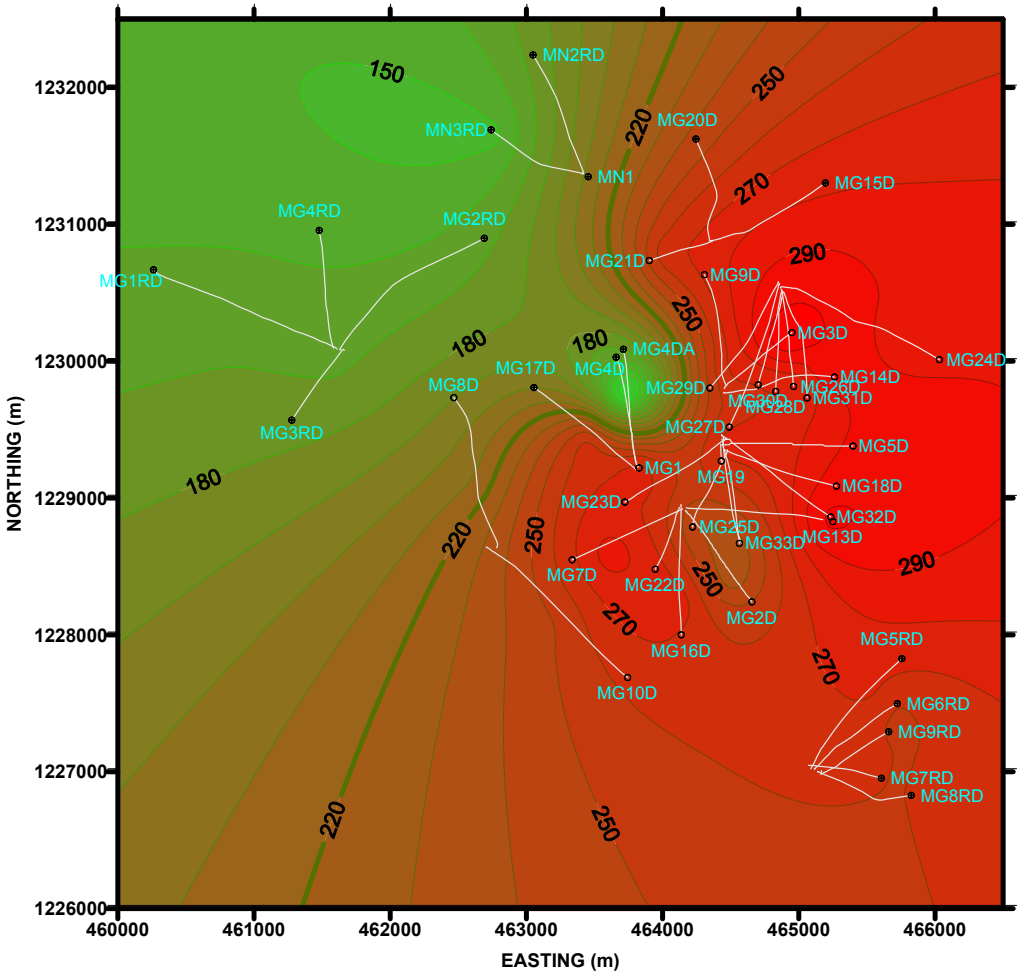

FIGURE 2: Mahanagdong 1997 baseline temperature contour at -1000 m a.s.l. (Mondejar et al., 2011)

In 2004, Pad MGF was developed with the objective of exploring the northeast region of Mahanagdong. New data obtained from drilled wells MG-38D (2004), MG-40D (2009), and MG-43D (2011), shown in Figure 3, led to an update of the conceptual model. These data were not yet available during the development of the baseline conceptual model. The other two wells drilled from the pad, MG-41D and MG-42D, were directed towards the existing production area and, hence, do not have a significant impact on the model's update. It must be noted that the latest well drilled in Pad MGF, MG-44D, was recently completed last September 2011, so data from this well were not included in this update of the conceptual model.

The updated conceptual model suggests a possible extension of the postulated upflow from the vicinity of wells MG-3D and MG-14D to include the area around wells MG-40D and MG-43D in the N-NE region of the field (Figure 4, showing a cross-section of the field directed along line AB in Figure 3). Furthermore, the relatively lower temperatures encountered in well MG-38D and the well's nil permeability delineated the resource boundary on the eastern part of the field. The upwelling fluids laterally outflow to the south at well MG-5RD and to the southwest of the area around well MG-1 as in the baseline model (Mondejar et al., 2011).

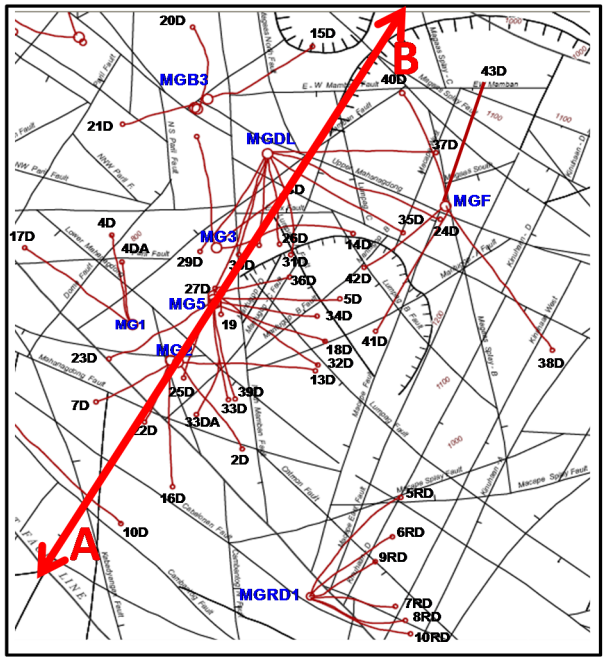

FIGURE 3: Mahanagdong updated well track map

Geochemical data indicate that a high-temperature, highly mineralized area was tapped in the N-NE region, exceeding the levels of the previously cited baseline upflow near wells MG-3D and MG-14D. Updated stable isotope data coupled with the temperature and reservoir chloride concentration of the fluids depict the upflow to be in the northeast part of the field which includes wells MG-37D, MG-40D, and MG-43D. Stable isotope values range from 0.1 to -1.16‰ $\delta^{18}O$ (where $\delta^{18}O$ expresses the relative difference of the isotope ratios between the sample and the standard), temperatures from the quartz geothermometer range from 290°C to 320°C, and reservoir chloride concentrations range from 2500 to 4400 mg/kg (Daco-ag, 2011).

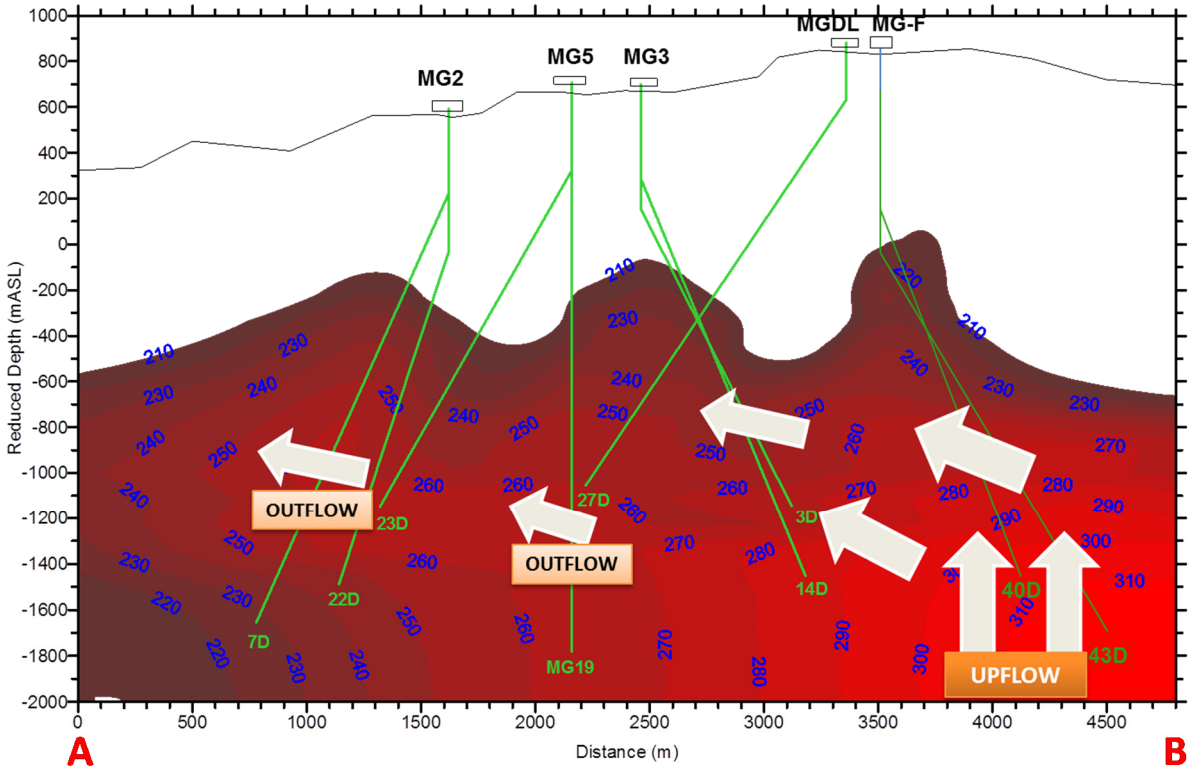

FIGURE 4: Mahanagdong updated conceptual model, using downhole temperatures measured from 2009 to 2011 (Mondejar et al., 2011)

It is worth mentioning that the process of updating the conceptual model of Mahanagdong has raised questions as to whether the N-NE region, characterized by wells MG-40D and MG-43D, is just an extension of the postulated upflow near wells MG-3D and MG-14D, or whether a separate heat source exists in this newly explored region (Angcoy, 2011). The question on whether a separate heat source exists in this region stems from the acidic chemistry of the fluids which contrast with the deep neutral brine system of the baseline upflow near wells MG-3D and MG-14D. Whether a separate heat source exists in the N-NE region still needs to be resolved.

2.3 Reservoir processes

Salonga et al. (2004) provided a thorough discussion of the processes and challenges induced by the large-scale production in Mahanagdong. The reservoir processes elucidated by Salonga et al. (2004) have been updated and further re-assessed by Daco-ag (2011) and Angcoy (2011) in their comprehensive reports on the changes in geochemical trends of Mahanagdong after ~15 years of production. Mondejar et al. (2011) reported the reservoir resource update, as well as an updated heat reserve estimate.

Since 1998, about a year after the start of commercial exploitation, in-situ steam provided by Mahanagdong wells was barely enough to meet the full load requirement of 180 MWe, even after drilling new wells and a workover of the existing wells. Continuous mass extraction has led to massive pressure drawdown of as much as 4.5 MPa in the central part of the field, where densely-spaced wells were drilled. On the other hand, slight overpressure was observed in the northern injection area of Pad MN1, while very minimal drawdown occurred in the southern injection area of Pad MGRD1. The presence of a thick cap rock in Mahanagdong prevented the development of an extensive steam zone because the fluids remain below the boiling-point-with-depth curve. Instead of phase separation, the depressurized central part invited an inflow of cooler fluids from peripheral areas.

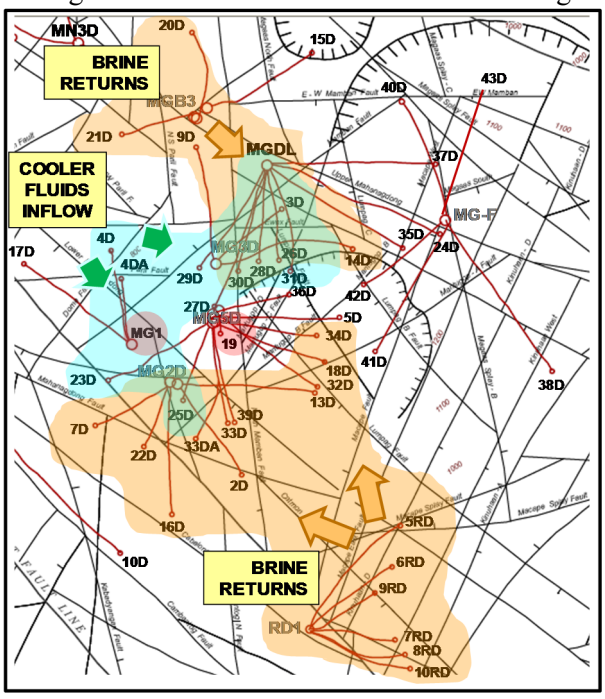

FIGURE 5: Major reservoir processes prevailing in Mahanagdong (modified from Belas-Dacillo et al., 2010)

The influx of peripheral fluids to the production area has resulted in field-wide cooling in Mahanagdong. Figure 5 shows the major processes affecting the field: (1) brine returns from Pad MGRD1 in the southern injection sink, (2) brine returns from Pad MGB3 in the northern injection sink, and (3) inflow of groundwater from the west. Among these processes, the inflow of groundwater fluids has been observed to have the most detrimental effect on the production sector.

In addition to these major reservoir processes, Mahanagdong is also beset with challenges contributing to the field's declining steam supply. These challenges include calcite blockages in some of its wells, and the presence of acidic fluid discharges, especially in wells located in the N-NE region of the field.

3. MAHANAGDONG TRACER TESTS

Several tracer tests have been conducted in Mahanagdong to define and establish connections between the injection and production wells. The following subsections will discuss the previous tracer tests conducted. Results of the 2003 NDS tracer test will be discussed quite extensively, as a correlation between the 2003 tracer test and the 2011 tracer test will later be discussed. A sound understanding of the 2003 tracer test results is necessary in order to fully appreciate the results of the 2011 tracer test. The procedure and context of the 2011 tracer test under study will also be discussed in this section.

3.1 Previous tracer tests

Sodium fluorescein was injected into well MG-4DA on October 1994, three years before the start of commercial exploitation, to determine if hydrological connections existed with the production wells. Tracer return was monitored in wells MG-1, MG-17D, MG-13D, and MG-16D. Results showed trace returns of sodium fluorescein in wells MG-13D and MG-16D, channelled through the Lower Mahanagdong Fault and then towards Mantugop Fault. The study warned of a potential problem if well MG-4DA was used as a reinjection well, especially at a very high load (Herras and Parrilla, 1995).

About two years after the start of commercial operation, another sodium fluorescein test was conducted in April 1999. The tracer was injected into well MG-17D, then a reinjection well used for disposing 70-90 kg/s of power plant condensate. A rapid tracer return of 48 hours and a much slower return of at least 20 days were monitored in wells MG-23D and MG-25D, respectively. Eight other monitored production wells did not show any tracer breakthrough. The Lower Mahanagdong Fault was identified to be the direct flow channel (Delfin et al., 2001). It should be mentioned that although fluorescein has the advantage of being detected at very low levels of concentration and can be measured easily, the main disadvantage of its use is that it decays at high temperatures. This thermal decay becomes significant above 200°C. At temperatures above 250°C, fluorescein decays too rapidly for it to be usable as a tracer (Axelsson et al., 2005).

Another tracer test was conducted in October 1999, this time using radioactive ^{125}I. Prior to conducting this tracer test, it was already known that wells MG-4DA and MG-17D in the western part of Mahanagdong were strongly affected by natural cold water incursion, as evidenced by downhole surveys, geochemical analysis, as well as petrologic evaluation of alteration minerals. With continuous field exploitation, steam supply steadily declined, with the influx of natural groundwater into the production sector cited as one of the significant contributory processes. It was deemed crucial to identify the flow path and flow rate of cooler groundwater to the production sector – the rationale for conducting the ^{125}I tracer test. Sixteen wells were monitored for more than 9 months, with only 6 wells (MG-26D/27D/28D/29D/30D/31D) – all located in Pad MGDL northeast of MG-4DA – showing positive tracer response. Only wells MG-29D and MG-27D yielded significant tracer recovery fractions of 11% and 13%, respectively. The postulated groundwater structural flow path was from the Mamban fault to North Mamban fault and towards the Ewex fault. The study concluded that under the field conditions at the time of the tracer test, the influx of groundwater to the production sector did not appear to be a major and immediate threat to resource sustainability of Mahanagdong (Delfin et al., 2001).

In 2003, three types of NDS tracers were utilized to define the hydrological flow paths of cooler peripheral fluids into the production sector and to assess the impact of their cooling effects. 1,6-NDS tracer was injected into well MG-4DA to trace the movement of natural groundwater. 1,5-NDS and 2,6-NDS tracers were injected into well MG-21D in the northern injection sink and well MG-5RD in the southern injection sink, respectively, to characterize the flow of injected brine to the production sector (Molina et al., 2005).

The 1,5-NDS tracer injected into well MG-21D at the northern injection sink yielded positive responses from 2 wells drilled in the northern part (MG-3D and MG-14D) and 3 wells in Pad MGDL (MG-

28D/30D/31D). Results showed profiles with sharp breakthrough curves which indicated high velocities, with breakthrough ranging from 2 to 11 days after injection or maximum velocities of 1300 to 3100 m/month, and low dispersion, implying an almost direct flow path of the fluids to the affected wells. Conduits of the injected brine were also major structures intersected by well MG-21D and the producing adjacent wells: i.e. the Malitbog, North Mamban and Ewex faults.

The 2,6-NDS tracer injected into MG-5RD at the southern injection sink yielded positive responses from 5 wells (MG-7D/16D/2D/22D/23D) in the southern area of the field. Fluids travel at moderately fast velocities, ranging from 20 to 56 days from injection or 215 to 600 m/month. The suggested flow channel was through the Catmon fault and then travelled through the Mahanagdong fault to reach the southern production wells.

The 1,6-NDS tracer injected into well MG-4DA in the western part of the field indicated positive responses from 2 wells drilled in the northern part (MG-3D and MG-14D) and 4 wells on Pad MGDL (MG-27D/29D/30D/31D), an almost similar trend to the 1,5-NDS responding wells. Results indicate a slow-moving fluid from well MG-4DA, with breakthrough in 56 to 114 days after injection or about 130 to 225 m/month.

Cooling predictions were conducted for all the tracer-responding wells, assuming the worst case scenario of a small surface area and pipe-like flow channels. Results from cooling predictions were then compared with the actual temperature decline. It was found that the predicted temperature declines were overall much lower than the actual temperature declines. This difference in the actual and predicted cooling was attributed to the masking of other possible reservoir processes (Herras et al., 2005); they will be evaluated later in this report.

3.2 2011 tracer test

Eight years after the 2003 tracer test, eleven more production wells (MG-34D/35D/36D/37D/38D/ 39D/40D/41D/42D/43D/44D) were drilled in Mahanagdong, with well MG-44D being completed just last September 2011. All of these wells, with the exception of wells MG-38D and MG-44D, were actively producing during the 2011 tracer test. To update the extent of the reservoir processes observed in the 2003 tracer test, the 2011 tracer test was conducted. Since most of the new wells were drilled in the central and northern areas of the field, the 2011 tracer test focused on studying the effect of brine returns from the northern injection sink, and the inflow of groundwater from the western part of the field.

Tracer injection was conducted from June 24 to 25, 2011. To evaluate the flow of brine returns from the northern injection sink to the production sector, three different types of NDS tracers were injected into three hot reinjection wells on Pad MGB3. To trace the extent of groundwater inflow in the west towards the production sector, another type of NDS tracer was injected into well MG-4DA. Details of the tracer injections are shown in Table 1. As shown in the table, well MG-4DA was shut throughout the tracer test duration except during tracer injection. This is because utilization of this well as a reinjection well has already been stopped for more than 5 years due to its detrimental effect on the production sector.

The mass of tracer injected was estimated by taking into account the reservoir volume, porosity, and detection limit of the analytical equipment used for the analysis. Tracer in powdered form was mixed with fresh water until sufficiently dissolved. Tracer solubility varies between the different tracers used. The tracer slurry was then injected into each well through the wing valve using a pump.

TABLE 1: Details of naphthalene disulfonate tracer injection

Tracer	Tracer amount (kg)	Injector well	Well location	Date injected	Well utilization	Average injection load (kg/s)
1,5-NDS	550	MG-21D	Pad MGB3, northern injection sink	24 June 11	Hot brine injection	46
2,6-NDS	550	MG-15D	Pad MGB3, northern injection sink	25 June 11	Hot brine injection	15
2,7-NDS	525	MG-20D	Pad MGB3, northern injection sink	24 June 11	Hot brine injection	110
1,6-NDS	550	MG-4DA	Pad MG1, western part of the field	25 June 11	Shut	-

Samples were collected from the two-phase lines through coiled stainless steel tubing connected at the bottom sampling points. The cooling coil was immersed in a cooling tub to ensure that the temperature of the sample was below 35°C. Samples were then acidified with acid volume equivalent to 1% of the collected sample volume. Sulfonate analysis was conducted using High Performance Liquid Chromatography (HPLC). Samples are considered representative of the two-phase mixture in each case.

For the first two weeks, sampling was done twice a day for the high priority wells, and three times a week for the low priority wells. From the 3rd to the 8th week, sampling was done once a day for high priority wells and twice a week for low priority wells. After the 8th week, sampling was reduced to once a week for high priority wells and twice a month for low priority wells. A total of 26 production wells were monitored and considered in the entire study duration (excluding well MG-44D which was not completed until September 2011). More than 900 samples were collected from the start of the tracer test until June 2012.

It must be noted that prior to tracer injection, water samples were collected from each of the monitoring stations for analysis of sulfonate baseline levels. It should also be pointed out that although the tracer recovery data utilized in this study only last up to June 2012 (one year after tracer injection), monitoring of tracer response in the production wells is still on-going as of this paper's writing.

4. TRACER TEST THEORY

Calculation of the total tracer mass recovered for each production well throughout the tracer test duration was done on the basis of the following equation:

$$m_i(t) = \int_0^t c_i(s) Q_i(s)\, ds \tag{1}$$

where $m_i(t)$ indicates the cumulative mass recovered as a function of time (t) in production well number i (kg), c_i indicates the tracer concentration (kg/l or kg/kg), Q_i the production rate of the well in question (l/s or kg/s), and s the integration variable (Axelsson et al., 2001).

The tracer breakthrough curve analysis was carried out using a one-dimensional flow-channel tracer transport model. This model assumes that the flow between injection and production wells may be approximated by one-dimensional flow, while flow channels could in fact be near-vertical fracture zones or parts of horizontal interbeds or layers. This one-dimensional tracer transport model is governed by the equation:

$$D \frac{\partial^2 C}{\partial x^2} = u \frac{\partial C}{\partial x} + \frac{\partial C}{\partial t} \tag{2}$$

where D is the dispersion coefficient (m^2/s), C the tracer concentration in the flow-channel (kg/m^3), x the distance along the flow channel (m), and u the average fluid velocity in the channel (m/s) given by $u = q/\rho A\phi$, with q the injection rate into the flow channel (kg/s), ρ the water density (kg/m^3), A the average cross-sectional area of the flow channel (m^2), and ϕ the flow-channel porosity.

In this simple model, molecular diffusion is neglected, with $D = \alpha_L u$ where α_L is the longitudinal dispersivity of the channel (m). Assuming instantaneous injection of a mass M (kg) of tracer at time t = 0, the solution is given by:

$$c(t) = \frac{uM}{Q}\frac{1}{2\sqrt{\pi Dt}}e^{\frac{-(x-ut)^2}{4Dt}} \tag{3}$$

where $c(t)$ is the tracer concentration in the production well fluid, Q the production rate (kg/s), and x the distance between the wells involved.

A detailed discussion of this one-dimensional tracer transport solution is provided in the paper by Axelsson et al. (2005). Subsequent modelling of the extent of cooling in the tracer-responding wells has been done using the analytical solution:

$$T(t) = T_0 - \frac{q}{Q}(T_0 - T_i)\left[1 - erf\left\{\frac{kxh}{c_w q\sqrt{\kappa(t - \frac{x}{\beta})}}\right\}\right] \tag{4}$$

$$\kappa = \frac{k}{\rho_r c_r} \tag{5}$$

$$\beta = \frac{qc_w}{\langle \rho c \rangle_f hb} \tag{6}$$

$$\langle \rho c \rangle_f = \rho_w c_w \phi + \rho_r c_r (1 - \phi) \tag{7}$$

where $T(t)$ is the production fluid temperature (°C), T_0 the initial reservoir temperature (°C), T_i the injection temperature (°C), q the injection rate (kg/s) in the flow channel, Q the production rate (kg/s), *erf* the error-function, k is the thermal conductivity of the reservoir rock (W/m °C), κ the thermal diffusivity of rock (m^2/s), and ρ and c are the density (kg/m^3) and heat capacity (J/kg °C) of water (w) and rock (r). In addition h and b are the vertical, or long, and horizontal, or short, sides of the flow-channel, respectively.

The analytical solution presented is for a flow-channel along a fracture zone or horizontal layer, which considers coupling between the heat advected along the flow-channel and the heat conducted from the reservoir rock to the fluid in the channel (Axelsson et al., 2005).

The ICEBOX software package (Arason et al., 2004) was employed in the tracer test calculations.

5. RESULTS AND DISCUSSION

5.1 Tracer recovery and first breakthrough

Since the 2011 tracer test was conducted mainly to update the extent of the inflow of cooler fluids to the production sector, the results and subsequent discussions of this study will be structured into two sections – response from the three types of NDS tracers injected in the northern injection sink which track injected brine returns, and response from the tracer injected in the western part of the field which tracks the groundwater inflow. As was stated in Chapter 3 of this report, the tracer data analysed in this

study only last up to June 2012, one year after the start of tracer injection. The background tracer concentration, detected in two of the monitored wells prior to the start of the tracer injection, was subtracted from the actual tracer concentration measured in these wells during the duration of this tracer study. The computer program TRMASS (Arason, 1993a) was used to calculate the cumulative mass of tracer recovered in each monitored well.

It is worth noting that for all four types of tracer injected, a significant number of monitored wells yielded only a single non-zero data point or only one instance of tracer breakthrough (Appendix I). These unconfirmed single instances of tracer breakthrough were not treated as positive tracer responses, and thus were not considered in the analysis.

5.1.1 Tracer recovery from the northern injection sink

Results of one year continuous monitoring for 2,6-NDS tracer injected in well MG-15D indicate that only one well, MG-41D, yielded a positive tracer response out of the 26 wells that were monitored. Well MG-41D was completed and connected to the system in the first half of 2010. This well was spudded in Pad MGF in the N-NE region of Mahanagdong, but directed towards the in-field production area (Figure 6).

The first tracer breakthrough detected in well MG-41D was 321 days after the start of tracer injection, with a very minimal tracer mass recovery of 0.05% (Table 2). There are only two detected instances of tracer breakthrough, 321 and 360 days after tracer injection (Figure 7). Tracer breakthrough was very slow, which implies an indirect and long flow-path from injector well MG-15D. The very minimal 2,6-NDS tracer recovery of 0.05% implies that almost all of the injected tracer was dispersed and diffused throughout the reservoir volume. Taken together, these results suggest that under the conditions during the tracer monitoring, reinjection in well MG-15D does not cause a significant return of reinjected brine as to have any appreciable thermal interference in the production sector. The two detected instances of tracer breakthrough in well MG-41D also suggest a possibility that the two data points are just noise, which all the more supports the contention that the brine reinjected in well MG-15D under the tracer test conditions had no appreciable impact on the production sector.

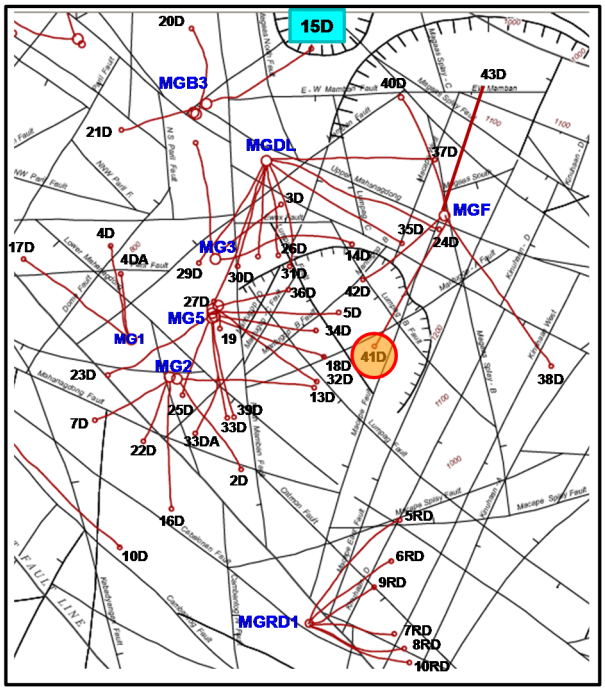

FIGURE 6: Location map of well MG-41D, the only 2,6-NDS tracer-positive well

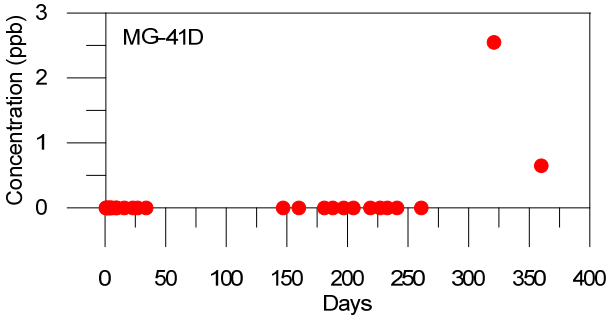

FIGURE 7: 2,6-NDS tracer (well MG-15D) recovery in well MG-41D

TABLE 2: 2,6-NDS (well MG-15D) mass recovery and time of first tracer breakthrough

Monitored well	Tracer recovery (%)	Time of first tracer breakthrough (days)	Peak tracer concentration (ppb)
MG-41D	0.05	321	2.55

The recovery of the 2,7-NDS tracer injected in well MG-20D showed positive responses in 4 of the 26 monitored wells. The location of these 4 positive wells (MG-14D, MG-23D, MG-27D, and MG-36D) is shown in Figure 8, along with the relative location of injector well MG-20D. The cumulative mass of 2,7-NDS recovered from all these wells is only 0.35%, with well MG-23D having the highest recovery among the 4 at 0.22% recovery (Table 3). Well MG-27D has only two detected instances of tracer breakthrough, with an almost nil recovery. However, since this well was intermittently shut and discharged throughout the tracer test, only a few samples were collected. Hence, the possibility of a more definitive and significant tracer recovery could not be discounted.

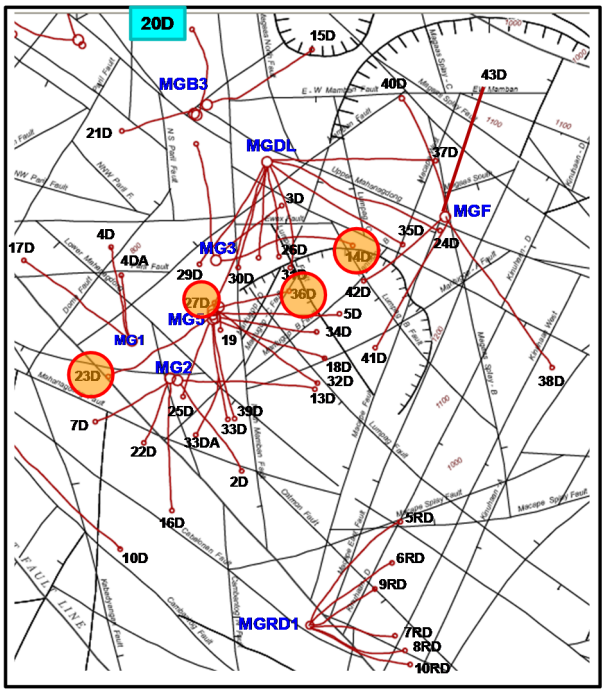

FIGURE 8: Location map of the 4 2,7-NDS tracer-positive wells

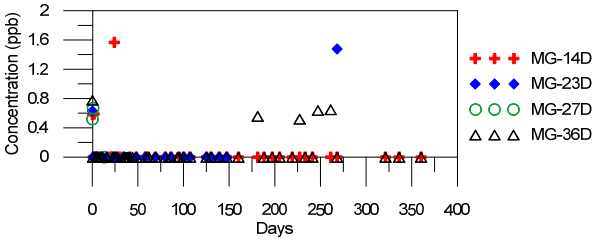

FIGURE 9: Tracer return profiles of 2,7-NDS tracer-positive wells

Table 3 also shows the time of the first 2,7-NDS tracer breakthrough detected in the monitored wells. As shown in the table, tracer breakthroughs in wells MG-23D, MG-14D, and MG-27D were deemed questionable because these breakthroughs were not confirmed by the next sample collected. The criteria used in considering the time of the first tracer breakthrough in this study was that the first instance of tracer detection must be confirmed by the next sample collected, as in the case of well MG-36D. Tracer return profiles of 2,7-NDS tracer-positive wells were highly indefinite with very few instances of tracer breakthrough (Figure 9). The tracer recovery profiles of the affected wells purport that flow-channels which seem to connect these affected wells to well MG-20D have very small flow-channel volumes, allowing only a minimal volume of fluids to pass through them. As a result, tracers that have been carried over these small flow-channel volumes have very low concentrations which could be below the detection limit. More than 99% of the injected tracer which has not been recovered is most likely diffused into the reservoir volume, although some tracer adsorption into the reservoir rocks cannot be ruled out. All of these results suggest that under the conditions during the tracer monitoring, reinjection of brine in well MG-20D does not pose any serious threat to the production wells.

TABLE 3: 2,7-NDS (well MG-20D) mass recovery and time of first tracer breakthrough

Monitored well	Tracer recovery (%)	Time of first tracer breakthrough (days)	Peak tracer concentration (ppb)
MG-23D	0.22	(?)	1.48
MG-36D	0.12	247	0.78
MG-14D	0.01	(?)	1.57
MG-27D	0	(?)	0.67

Injection of 1,5-NDS tracer in well MG-21D yielded 5 wells with positive responses out of the 26 monitored wells. These tracer-positive wells (MG-36D, MG-24D, MG-34D, MG-41D, and MG-42D) are shown in Figure 10.

TABLE 4: 1,5-NDS (well MG-21D) mass recovery and time of first tracer breakthrough

Monitored well	Tracer recovery (%)	Time of first tracer breakthrough (days)	Peak tracer concentration (ppb)
MG-34D	0.17	(?)	2.79
MG-36D	0.14	17	1.98
MG-24D	0.07	(?)	0.94
MG-42D	0.04	(?)	1.35
MG-41D	0.01	198	0.94

The cumulative 1,5-NDS tracer recovery is very low at only 0.43%, with the highest recovery in well MG-34D at a mere 0.17% (Table 4). As with the case of 2,7-NDS tracer-positive wells, three wells (MG-34D, MG-24D, MG-42D) had questionable rapid tracer breakthroughs. For well MG-41D, the tracer was first detected after 198 days. There are only two detected instances of tracer recovery, with almost nil total recovery of 0.01% (Figure 11). This implies an indirect and long flow-channel from injector well MG-21D to well MG-41D. Of the five tracer-positive wells, MG-36D appears to have the most definitive tracer recovery (Figure 12), characteristic of a tracer return curve. Inverse modelling will be conducted for this tracer return curve to estimate important flow-path parameters, as will be demonstrated in the succeeding section.

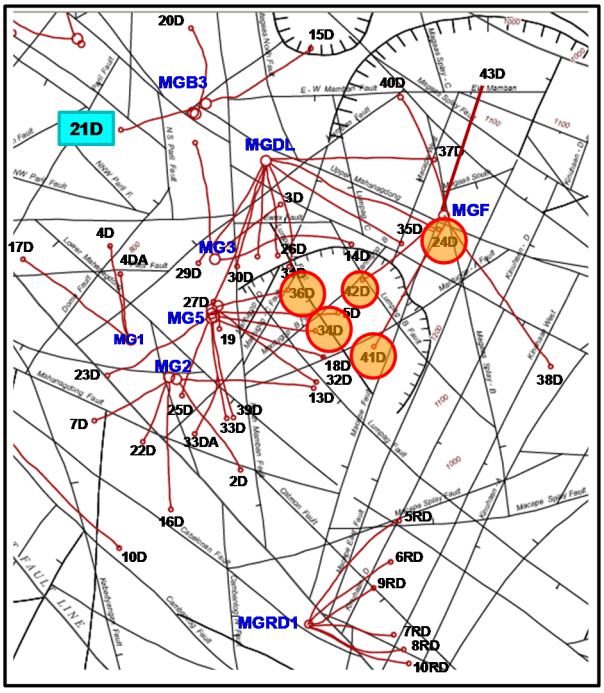

FIGURE 10: Location map of the 51,5-NDS tracer-positive wells

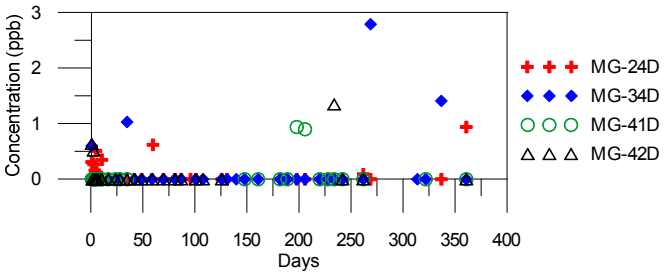

FIGURE 11: 1,5-NDS tracer-positive wells with incomplete tracer return profiles

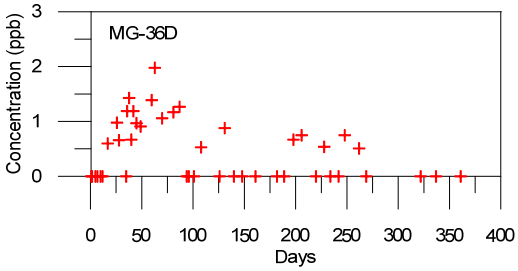

FIGURE 12: 1,5-NDS tracer return profile of MG-36D

5.1.2 Tracer recovery from MG-4DA in the west

Tracer recovery monitoring of 1,6-NDS tracer injected in well MG-4DA produced quite disquieting results as 13 of the 26 monitored wells yielded positive returns (Figure 13) with a total tracer mass recovery of 23.4%. That a majority of these positive tracer responses had relatively high recoveries and very fast breakthroughs is also alarming, especially since no actual water injection was done into well MG-4DA since the well was shut in throughout the entire tracer test duration (Table 5). In less than 50 days, tracer was already detected in 8 of the tracer-positive wells. Well MG-36D had the highest

recovery at 8.21%, while well MG-27D had the lowest recovery owing to the fact that for this well only three samples were collected during the entire tracer study. If more samples were collected for well MG-27D, tracer recovery could be higher. For well MG-28D, the time of the first tracer breakthrough could not be determined because the well was shut from July 2011 and sampling started later in December 2011 after the well was discharged. The tracer return profiles of 9 of the tracer-positive wells appear to be definitive and to exhibit characteristic tracer return curves (Figure 14), while 4 of the tracer-positive wells appear to have incomplete tracer return curves (Figure 15). A separate discussion on the modelling and implications of these tracer return profiles is presented in the next section.

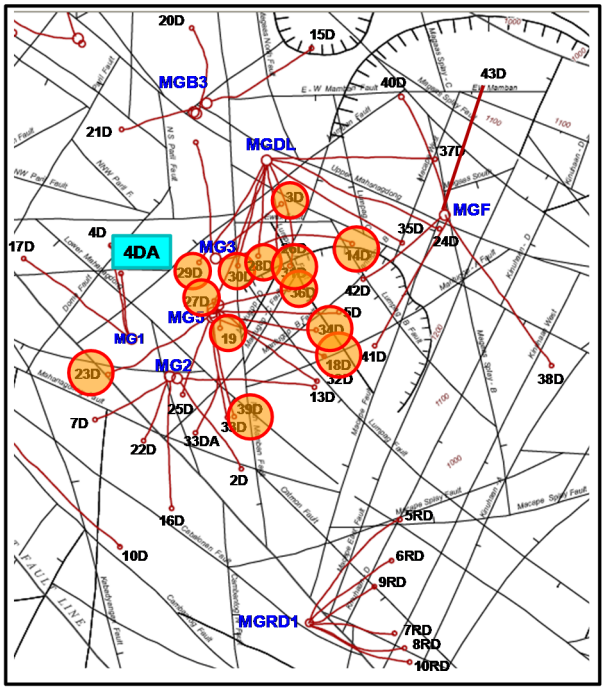

FIGURE 13: Location map of the 13 1,6-NDS tracer-positive wells

5.2 Inverse modelling of tracer response

Tracer return profiles could be simulated to provide an estimate of the reservoir parameters involved in the one-dimensional tracer transport

TABLE 5: 1.5-NDS (well MG-21D) mass recovery and time of first tracer breakthrough

Monitored well	Tracer recovery (%)	Time of first tracer breakthrough (days)	Peak tracer concentration (ppb)
MG-36D	8.21	6	111
MG-31D	5.38	23	24.3
MG-18D	2.23	34	15.6
MG-29D	2.18	24	22.9
MG-23D	1.96	7	26.1
MG-30D	0.96	41	10.7
MG-3D	0.68	46	6.06
MG-14D	0.64	34	10.5
MG-19	0.43	147	7.18
MG-34D	0.37	139	12.7
MG-28D	0.21	-	8.65
MG-39D	0.13	86	1
MG-27D	0.01	(?)	2.13

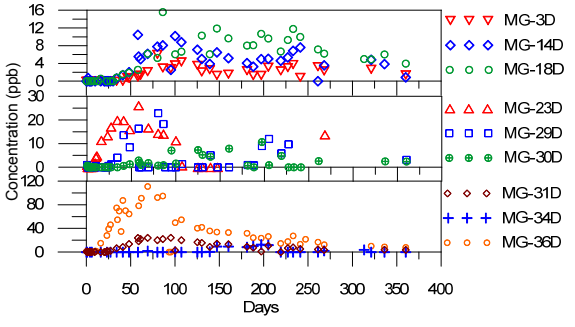

FIGURE 14: 1,6-NDS tracer-positive wells with good tracer return profiles

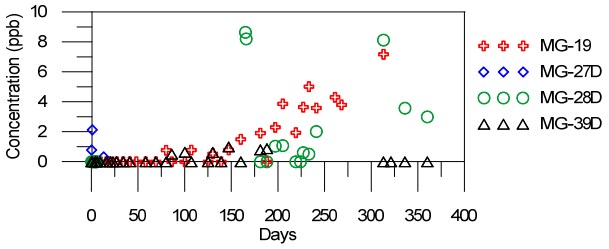

FIGURE 15: 1,6-NDS tracer-positive wells with incomplete tracer return profiles

model discussed in Chapter 4. To model the tracer return profiles, the computer code TRINV (Arason, 1993b) was used. By first providing an initial guess of the model parameters, TRINV automatically simulates the data through inversion. TRINV uses non-linear least-squares fitting to simulate the data and obtain model properties (Axelsson et al., 2005).

5.2.1 Inverse modelling of tracer break-through curves from the northern injection sink

In general, tracer return profiles from the three reinjection wells in the northern injection sink (MG-15D, MG-20D, and MG-21D) do not exhibit the characteristic tracer return profile which resembles the shape of a bell curve. Tracer monitoring of the three NDS tracers injected in the northern injection sink yielded sparse data points and consequently do not provide good quality data for inverse modelling. Of all the tracer-positive wells affected by injection in the northern injection sink (1 well for 2,6-NDS injected into well MG-15D, 4 wells for 2,7-NDS injected into well MG-20D, and 5 wells for 1,5-NDS injected into well MG-21D), only the tracer return profile of well MG-36D (Figure 12) from 1,5-NDS tracer allowed for a reliable data simulation.

Figure 16 shows the simulated tracer return profile of well MG-36D. As shown in the figure, a one-channel flow would yield a reasonable fit given the disperse data points. The estimated properties of the flow channel are shown in Table 6. Results for the simulation indicate that a mere 0.17% of injected fluids from well MG-21D would travel towards well MG-36D at a moderate speed of 498 m/month undergoing high dispersion, as suggested by the high dispersivity of the flow-channel.

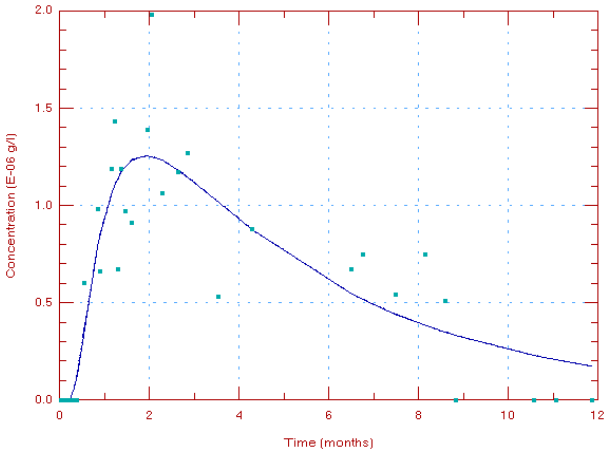

FIGURE 16: Observed and simulated 1,5-NDS tracer recovery in well MG-36D

TABLE 6: Model parameters used in simulating the 1,5-NDS tracer recovery in well MG-36D

Well	Channel length, x (m)	Mean velocity, u (m/month)	Area×porosity, $A\phi$ (m^2)	Dispersivity, α_L (m)	Mass recovery (%)
MG-36D	1499	498	0.54	703	0.17

5.2.2 Inverse modelling of tracer breakthrough curves from well MG-4DA in the west

Modelling of tracer return profiles of the 1,6-NDS tracer-positive wells from well MG-4DA were not as straightforward as that of the 1,5-NDS tracer recovery in well MG-36D. In the case of 1,5-NDS tracer injected into well MG-21D, the injection rate of well MG-21D was known throughout the tracer test's duration. On the contrary, the only time that well MG-4DA had actual fluid injection from the surface was during the time of tracer injection, after which well MG-4DA was shut. This poses a problem as to what injection rate to use for the simulation.

Prior to commercial exploitation, wells MG-4DA and MG-17D had already been identified as being strongly affected by natural groundwater inflow. The effect of this groundwater downflow in the wellbore is marked by the abrupt temperature reversal from 230 – 240°C to 170 – 180°C. Although a workover had been conducted to cement plug and case-off the downflow zone, the downflow still persisted. This strong downflow made the wells unfit for production. Delfin et al. (2001) reported that through a flowmeter shut-in survey conducted in 1990, the downflow in well MG-4DA had been estimated to be about 3.4 kg/s. Another flowmeter shut-in survey was conducted in well MG-17D, a nearby well, and the downflow for this well had been estimated to be about 7 kg/s. Delfin et al. (2001)

then asserted that it is reasonable to assume that the total flow rate of natural groundwater in the two wells is at least 10 kg/s.

The natural groundwater values indicated by Delfin et al. (2001) were used as the injection rate of well MG-4DA in the simulation. Two injection rate scenarios were simulated: an optimistic scenario where the injection rate is 3.4 kg/s, and a pessimistic one where the injection rate is 10 kg/s. The need to come up with a pessimistic scenario arose due to the fact that as continuous mass extraction has been going on for years since the flowmeter survey, massive reservoir pressure drawdown may have aggravated this downflow in well MG-4DA.

Of the 13 1,6-NDS tracer-positive wells, 9 wells were simulated. The other 4 tracer-positive wells (MG-19, MG-27D, MG-28D, MG-29D) did not provide satisfactory data for inverse modelling (Figure 15). The simulated tracer return profiles of these 9 wells are shown in Figure 17. As shown in Figure 17, a two-channel flow produced a better fit for 3 wells (MG-36D, MG-3D, and MG-14D) while the rest of the wells only employed a one-channel flow. Table 7 shows the model parameters used in the simulation. It is noticeable in the table that there are two values for the parameter Aϕ (area×porosity), one value calculated at the optimistic well MG-4DA downflow rate q = 3.4 kg/s, and the other at a downflow rate of q = 10 kg/s. These two values of the parameter Aϕ will later be used in modelling the thermal interference and to predict the degree of cooling in the tracer-positive production wells.

The cross-plot of mean velocity and tracer mass recovery in Figure 18 shows 6 wells with recoveries in their flow-channels greater than 1%, while the remaining 3 wells (MG-3D, MG-14D, and MG-34D) have very small recoveries of less than 1%. Well MG-36D appears to have the highest recovery (7.8%)

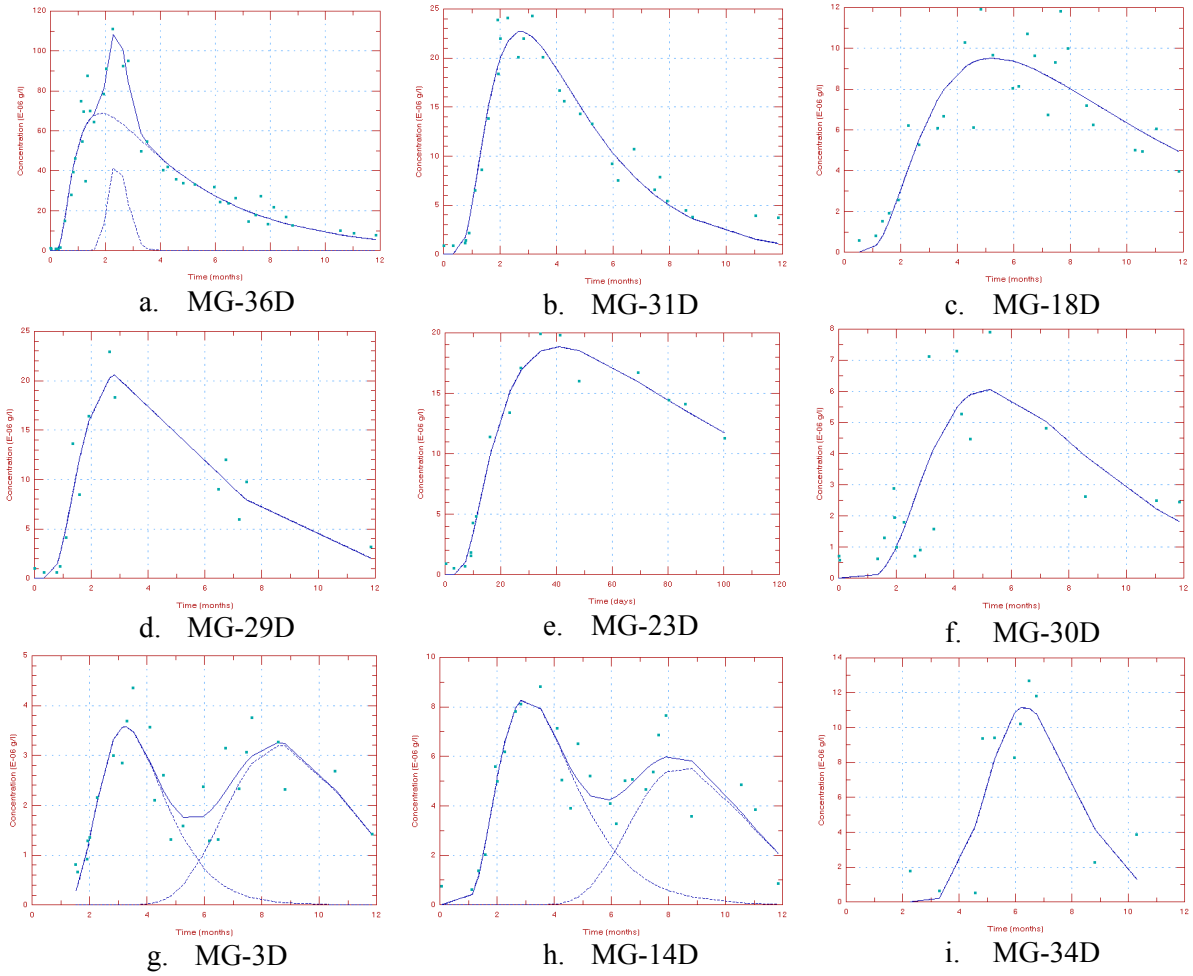

FIGURE 17: Observed and simulated 1,6-NDS tracer recovery from MG-4DA

in one of its flow-channels, while the second-flow channel has minimal recovery at 0.8%. It is worth noting that although the second flow-channel has minimal recovery, it has faster mean velocity and lower dispersivity which means that it channels fluids faster than the main flow-channel. Mean velocities range from 132 to 533 m/month, but the average lies near 300 m/month.

TABLE 7: Model parameters used to simulate the 1,6-NDS tracer recovery in the 9 tracer-positive wells

Well	Channel length, x (m)	Mean velocity, u (m/month)	Area×porosity, Aϕ (m^2) at q = 10 kg/s	Area×porosity, Aϕ (m^2) at q = 3.4 kg/s	Dispersivity, α_L (m)	Mass recovery (%)
MG-36D	776	288	9.29	3.16	305	7.79
	1208	496	0.55	0.19	11.0	0.79
MG-31D	1416	426	4.55	1.55	280	5.65
MG-18D	1338	198	5.40	1.84	337	3.11
MG-29D	921	245	4.60	1.56	201	3.28
MG-23D	410	200	3.08	1.08	181	1.80
MG-30D	1244	207	2.03	0.69	180	1.23
MG-3D	1294	146	1.09	0.37	39.0	0.46
	1009	294	0.33	0.11	61.0	0.28
MG-14D	1775	533	0.22	0.08	164	0.35
MG-34D	1146	132	0.88	0.30	33.0	0.34
	1423	219	0.58	0.20	40.0	0.37

Another cross-plot, shown in Figure 19, shows the relative tracer recoveries for each flow channel but, this time, plotting the dispersivity values instead of mean velocities. An interesting trend is revealed in the figure which suggests that wells with higher tracer recoveries tend to have a higher degree of dispersion while wells with lower recoveries tend to have lower dispersivity. The cross-plot of $A\phi$ and tracer mass recovery (Figure 20) has a similar trend with that of dispersivity, i.e. the higher the tracer mass recovery, the greater the value of $A\phi$, though it could be viewed the opposite way, in which case the higher the value of available $A\phi$ for fluid flow, the higher the expected tracer mass recovery. It appears that the higher value of $A\phi$ leads to more space for tracer dispersion, thus a higher value of dispersivity. Dispersivity values range from 11 to 337 m, but the average lies near 150 m.

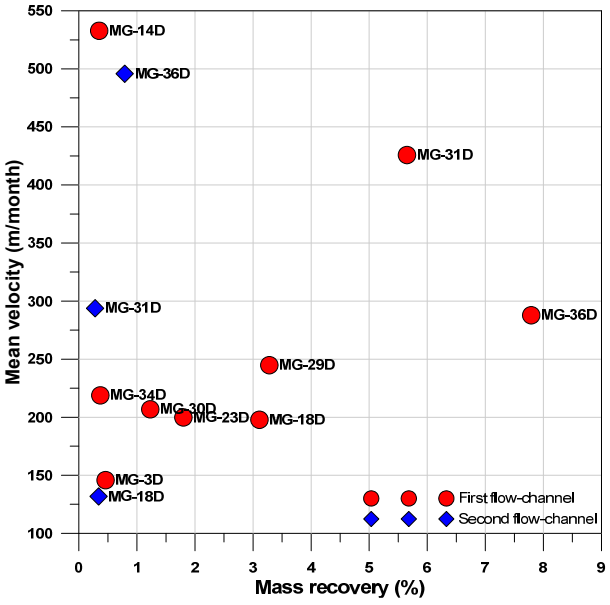

FIGURE 18: Cross-plot of mean velocity and tracer mass recovery for the 9 1,6-NDS tracer-positive wells

5.3 Thermal interference modelling

The main purpose of modelling tracer return profiles is not just to establish the hydrological connection between the injector and monitored wells and estimate the flow-channel parameters. It is equally important to estimate the degree of thermal interference in the affected production wells. To model the degree of cooling due to long-term reinjection, the computer code TRCOOL (Axelsson et al., 1994) was employed, which is based on Equation 4.

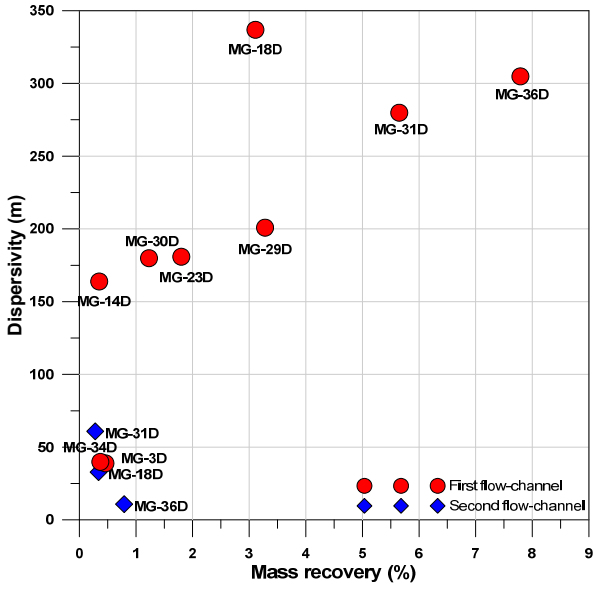

FIGURE 19: Cross-plot of dispersivity and tracer mass recovery for the 9 1,6-NDS tracer-positive wells

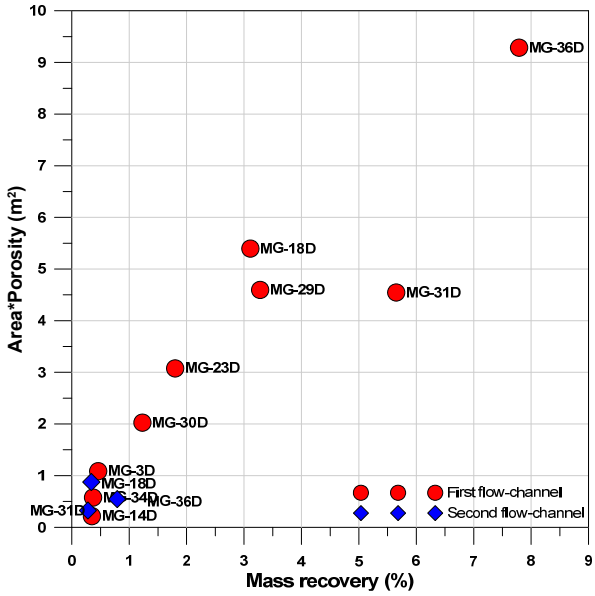

FIGURE 20: Cross-plot of area×porosity and tracer mass recovery for the 9 1,6-NDS tracer-positive wells

Model parameters derived from inverse modelling of tracer return profiles were used as input in TRCOOL. By assuming a certain value for flow-channel porosity, the flow-channel cross-sectional area can be calculated from the model parameter Aϕ. In this case, 20% porosity was used based on the average porosities of tracer-positive wells in the current numerical model of Mahanagdong. To obtain a conservative cooling prediction, the worst case scenario of equal height and thickness of flow-channels was assumed. The effect of a 20-year reinjection scenario was predicted, up to the year 2031, at which time the Leyte Renewable Energy Contract expires.

5.3.1 Thermal interference model of well MG-36D from 1,5-NDS tracer injected in well MG-21D

Figure 21 shows the predicted degree of cooling of well MG-36D due to an average reinjection of 46 kg/s of 170°C brine into well MG-21D. The thermal interference model indicates that a long-term reinjection of 46 kg/s for 20 years will cause a minimal temperature decline of ~0.05°C. Different reinjection load scenarios for well MG-21D were simulated to determine the degree of cooling in well MG-36D (Figure 22). The maximum measured reinjection capacity of well MG-21D is 137 kg/s

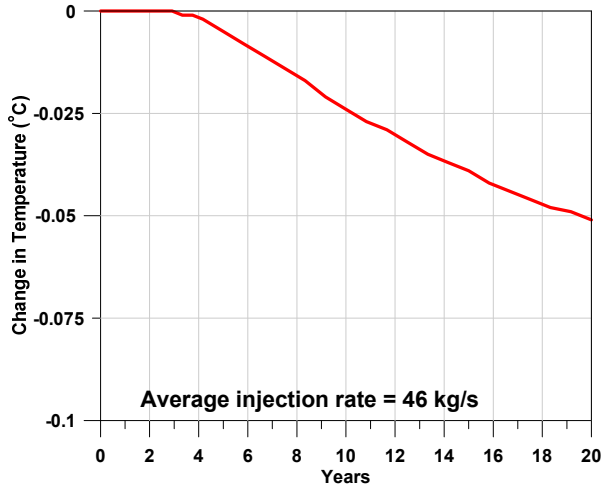

FIGURE 21: Predicted degree of cooling of well MG-36D due to reinjection of 170°C brine into well MG-21D

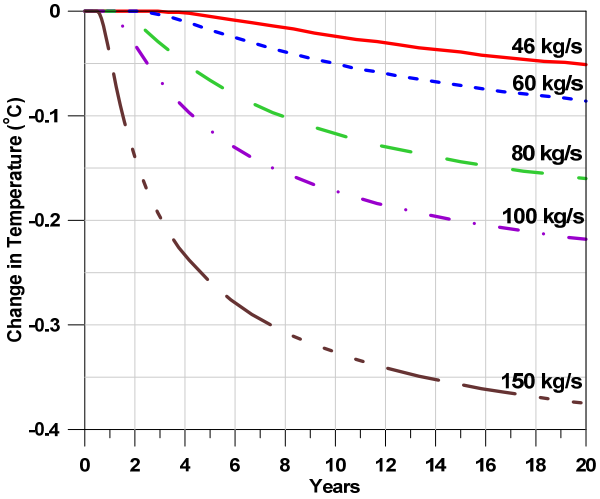

FIGURE 22: Predicted degree of cooling of well MG-36D at different MG-21D reinjection rates

(February 2009 tracer flow measurement), so the simulations in Figure 22 present a reinjection scenario of up to 150 kg/s. Results suggest that even at 150 kg/s reinjection load, the expected degree of cooling in well MG-36D will be about 0.4°C. These findings support the idea put forward in Section 5.1.1 that, under the conditions during the tracer test duration, reinjection in the northern injection sink has no appreciable thermal effect on the production sector.

5.3.2 Thermal interference modelling of 1,6-NDS tracer-positive wells from well MG-4DA

Unlike well MG-21D which has known brine injection rate, well MG-4DA was shut throughout the tracer test duration. As a result, two cooling scenarios will be presented for each tracer-positive well – an optimistic scenario with a natural downflow rate of 3.4 kg/s, and a pessimistic scenario of 10 kg/s downflow. Table 8 shows the predicted degree of cooling of the 9 1,6-NDS tracer-positive wells which were modelled in Section 5.2.2, while the plots of how temperature declines with time for each well is shown in Appendix II.

As shown in Table 8, the pessimistic scenario of a 10 kg/s downflow rate in well MG-4DA purports that well MG-36D will have the highest predicted temperature decline of 1.4°C in 20 years. All other wells have negligible temperature decline based on the model.

TABLE 8: Predicted degree of cooling of 1,6-NDS tracer-positive wells after 20 years

Production well	Degree of cooling (°C)	
	Optimistic	Pessimistic
MG-36D	0.4	1.4
MG-31D	0.1	0.4
MG-18D	0	0.2
MG-29D	0.1	0.3
MG-23D	0.1	0.3
MG-30D	0	0
MG-3D	0	0
MG-14D	0	0
MG-34D	0	0

5.4 Groundwater inflow modelling

Results of the thermal interference modelling of the 1,6-NDS tracer-positive wells indicate that with well MG-4DA shut and with the well's pessimistic natural downflow rate of 10 kg/s, only well MG-36D will have an appreciable temperature decline after 20 years. Since well MG-4DA has been shut for more than 5 years already, it makes sense to compare the actual degree of cooling of the 1,6-NDS tracer-positive wells with the predicted temperature decline from the model. A close agreement between the actual and predicted temperature decline would impart confidence and credibility to the current understanding of the effect of groundwater inflow from the western part of the field. However, a significant gap between the actual and predicted temperature decline would suggest the occurrence of other factors and processes.

Table 9 shows the actual measured cooling in 9 years (from 2003 to date) in comparison with the predicted cooling after 20 years (until 2031). The reference time for the actual cooling was chosen to be the year 2003 since that was the year of the last tracer test, after which reinjection strategies were implemented to manage the inflow of peripheral fluids to the production sector. Data of actual measured cooling from 2003 to date indicate that actual temperature decline in all the affected wells is much greater than the predicted temperature

TABLE 9: Comparison of predicted and actual temperature decline

Production well	Predicted cooling after 20 years (°C)		Actual cooling in 9 years (since 2003) (°C)
	Optimistic	Pessimistic	
MG-36D	0.4	1.4	11
MG-31D	0.1	0.4	8
MG-18D	0	0.2	6
MG-29D	0.1	0.3	14
MG-23D	0.1	0.3	3
MG-30D	0	0	10
MG-3D	0	0	1
MG-14D	0	0	6
MG-34D	0	0	10

decline, even after 20 years. This finding is quite interesting as this suggests that other factors are at play which could cause a greater temperature decline than that predicted by the model.

It must be stressed at this point that the predicted cooling from the model is based on the 1,6-NDS tracer recovery profiles. What this means is that inherent in the calculation of cooling effect is the assumption that the cause for the predicted cooling in Table 9 is the percentage of well MG-4DA (represented by the tracer recovery) downflow that has reached the production well. The model predicts that even at the pessimistic MG-4DA downflow rate of 10 kg/s, a maximum cooling of 1.4°C (for well MG-36D) is expected. This is clearly not the case, as the comparison with the actual cooling shows.

Monitoring of the physical and chemical parameters of the affected wells through time indicates that colder fluid of groundwater character is causing the actual temperature decline. Decline in enthalpy and steam flow, as well as difficulty in maintaining commercial wellhead pressures for the majorly affected wells, suggests that the groundwater inflow to the production sector has a much larger scale and magnitude than the downflow measured in well MG-4DA. It could even be stated that, aside from the natural groundwater downflow from well MG-4DA that the tracer test was able to confirm and quantify, there is an even greater quantity of groundwater that is flooding the production sector as a result of massive pressure drawdown.

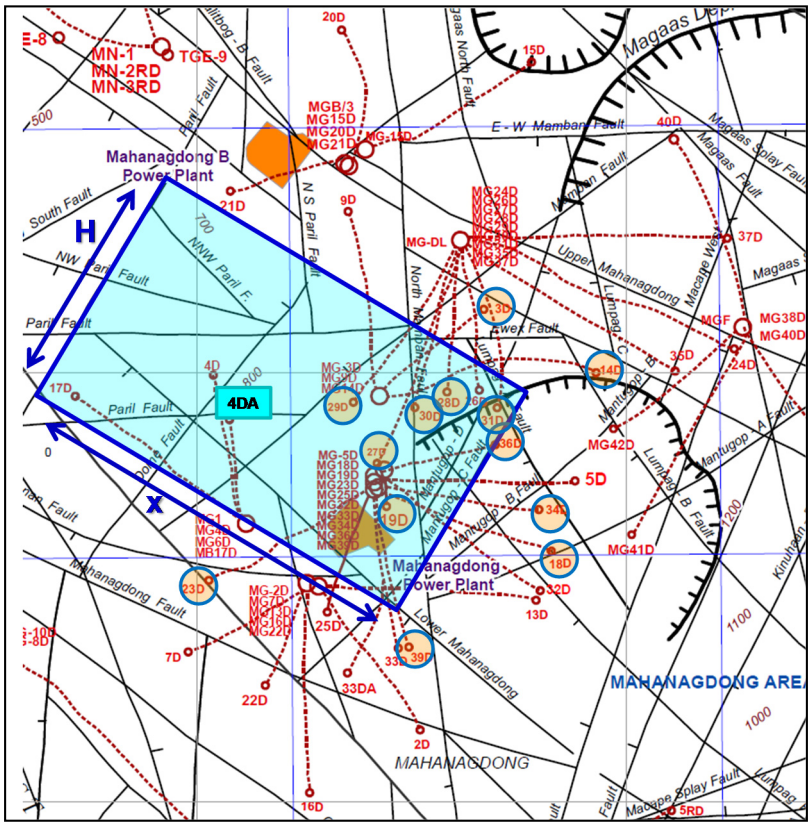

FIGURE 23: One-dimensional rectangular slab groundwater flow-path model

To estimate this general groundwater inflow (in addition to the downflow in wells MG-4DA and MG-17D), a one-dimensional rectangular slab groundwater flow-path model was set up (Figure 23). The model is oriented in a northeast to southwest direction as this is the inferred direction of the groundwater based on the principal structural conduits and temperature contour (Figure 2). As shown in Figure 23, H is the width of the rectangular slab model, which was aligned with the direction of the Paril fault – a major conduit of groundwater. The distance of the production wells from H is represented as x. These two parameters, together with the slab thickness b and the groundwater flow rate q will be varied to find the best fit for the actual temperature decline in the production wells. As with the thermal interference modelling conducted in Sections 5.3.1 and 5.3.2, the computer code TRCOOL was employed in modelling the groundwater inflow.

The temperature decline with time of five 1,6-NDS tracer-positive wells was used to calibrate the groundwater inflow model. These five wells were deemed to be the most affected production wells based on output decline, physical and chemical parameters, and results of the current tracer test. Four of these wells are on Pad MGDL (MG-27D, MG-29D, MG-30D, and MG-31D) and were already online

since the start of commercial exploitation in 1997, while the fifth well is a make-up and replacement well (MG-36D) that was completed in 2004. These five wells were drilled within the central production area where wells are densely-spaced and pressure drawdown the highest. The start of commercial exploitation in 1997 served as the reference time in modelling the inflow of groundwater.

Figure 24 shows the results of the groundwater inflow modelling simulations. The simulated temperature decline for all 5 wells generally matched the actual temperature decline. For well MG-27D, a single model was not able to yield a good match with the actual temperature decline, owing to a very rapid decline starting in the 11th year. In order to produce a good match, a second model (Model B) was introduced to simulate this faster temperature decline. Note that by using Model A from the start of commercial exploitation until the 10th year, and adding the response of Model B from the 11th year onwards, a very good match between the actual and simulated temperatures was observed. Model B for well MG-27D could suggest an additional flow-channel which has a greater rate of groundwater inflow, causing a more rapid decline in temperature than the first channel (Model A).

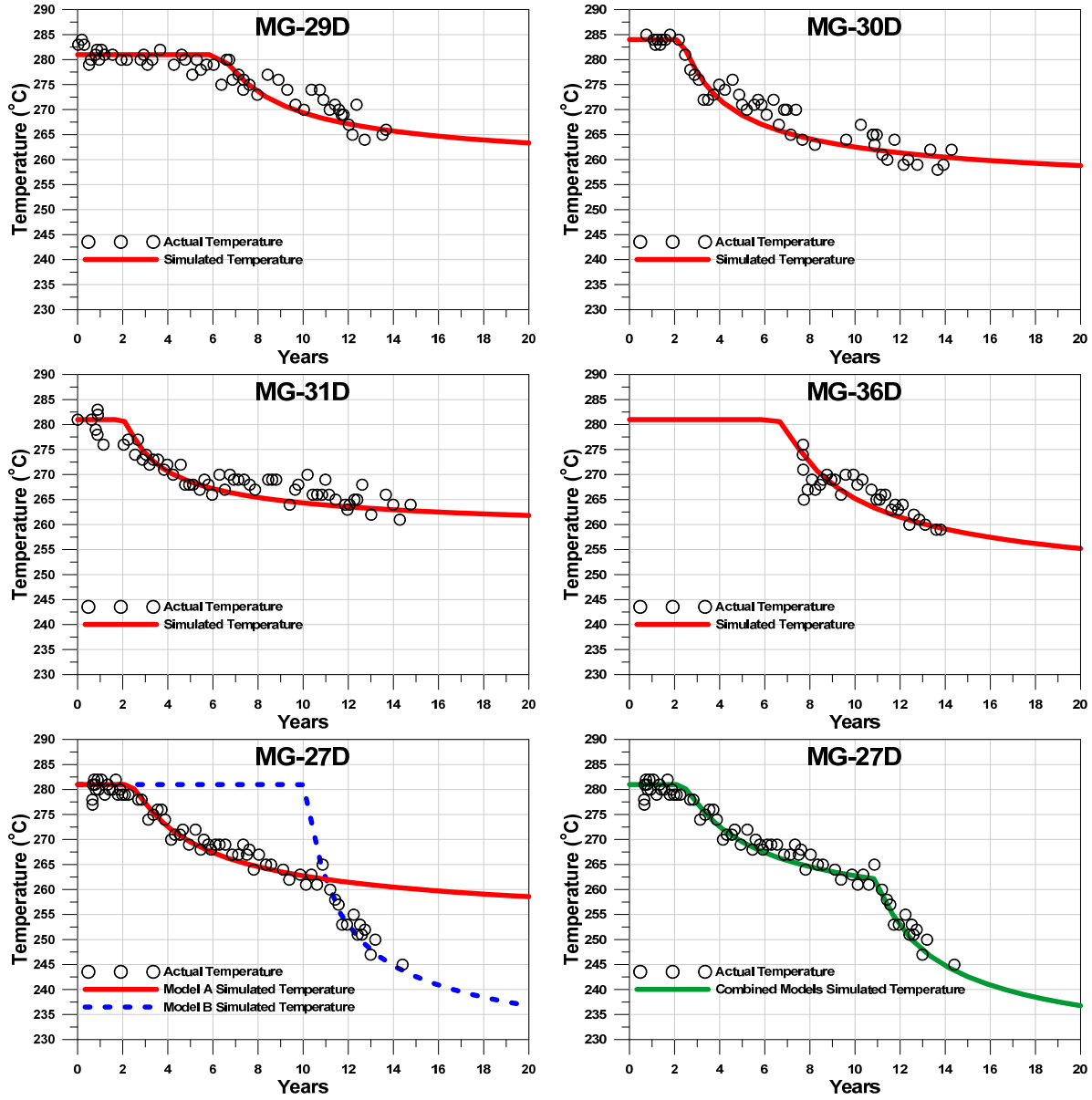

FIGURE 24: Groundwater inflow modelling results showing the actual and simulated temperatures with time of the 5 most affected production wells

The model parameters for each of the simulated production wells in Figure 24 are shown in Table 10. As previously mentioned, the main goal in modelling the groundwater inflow is to have an estimate of its flow rate. By using the average production rate, the initial reservoir temperature of each well, and groundwater temperature as input parameters, the flow-channel dimensions (x, b, and H) as well as the groundwater inflow rate have been varied to fit the actual temperature decline. The model parameters summarized in Table 10 indicate that the rectangular slab flow-path model in Figure 23 has a thickness in the range of 10-25 m, a width of 1000-1700 m, and distance from the groundwater source of 1500-2000 m. The rate of groundwater inflow to the production sector is estimated to be around 200-300 kg/s.

TABLE 10: Model parameters for each simulated production well

Parameter	MG-29D	MG-30D	MG-31D	MG-36D	MG-27D (Model A)	MG-27D (Model B)
Thickness, *b* (m)	25	10	10	25	8	61
Width, *H* (m)	1450	1150	1000	1700	1421	1660
Distance, *x* (m)	1500	2000	1600	2020	1950	2050
Groundwater inflow rate, *q* (kg/s)	200	250	190	300	245	460
Average reservoir production rate, *Q* (kg/s)	900	900	900	900	900	900
Initial reservoir temperature, *T* (°C)	281	284	281	281	281	281
Groundwater temperature, T_g (°C)	165	165	165	165	165	165

Aside from estimating the groundwater flow-path dimensions and the groundwater inflow rate, it is also important to somehow estimate the velocity at which it encroaches on the production sector. Estimating the groundwater velocity will provide valuable insight into its relative speed compared to the modelled fluid mean velocity from well MG-4DA to the affected production well as discussed in Section 5.2.2. Table 11 shows the respective velocities of the groundwater inflow and the fluids from well MG-4DA. Groundwater inflow has an average velocity of ~200 m/month and a standard deviation of 120 m/month, while fluids from well MG-4DA have an average velocity of ~300 m/month with a standard deviation of 95 m/month. The general groundwater velocity could therefore be expressed as 195 $\pm$ 120 m/month while that of well MG-4DA fluids as 292 $\pm$ 95 m/month. The relatively large values of standard deviation in both the velocities of groundwater inflow and well MG-4DA fluids reflect variations in the velocity which depend upon the location in the slab. Velocity variations could also be a result of variations in slab dimensions and properties, as well as the uncertainty in the estimates arising from the simplicity of the model. The fact that the calculated velocities of 195 $\pm$ 120 m/month and 292 $\pm$ 95 m/month are within each other´s standard deviations implies that the tracer carried by the downflow in

TABLE 11: Estimated groundwater velocity to the production sector compared with the mean velocity of the fluids from well MG-4DA to the affected production wells

	MG-29D	MG-30D	MG-31D	MG-36D	Average velocity (m/month)	Standard Deviation (m/month)
Calculated groundwater velocity towards the production sector (m/month)	81	317	277	103	195	120
Mean velocity of the fluids from well MG-4DA to the affected production wells (m/month)	245	207	426	288	292	95

the wells travels with the general groundwater flow as well. In effect, the downflow observed in well MG-4DA could most likely be just a small part of a much greater groundwater inflow towards the production sector, estimated to be around 200 – 300 kg/s.

5.5 Correlation with 2003 tracer test

Now that the results of the 2011 Mahanagdong tracer test have been presented, it is imperative to correlate the present tracer test results with the results of the previous tracer test conducted in 2003. The major reason for doing this comparison is to update the extent of the reservoir processes, especially that of the groundwater inflow.

Figure 25 shows the extent of brine returns in both the 2003 and 2011 tracer tests. Note that in the 2003 tracer test, only well MG-21D was injected with tracer in the northern injection sink while another tracer was injected in well MG-5RD in the southern injection sink. In the 2011 tracer test, three reinjection wells in the northern injection sink were injected with tracers while no tracer was injected in the southern injection sink.

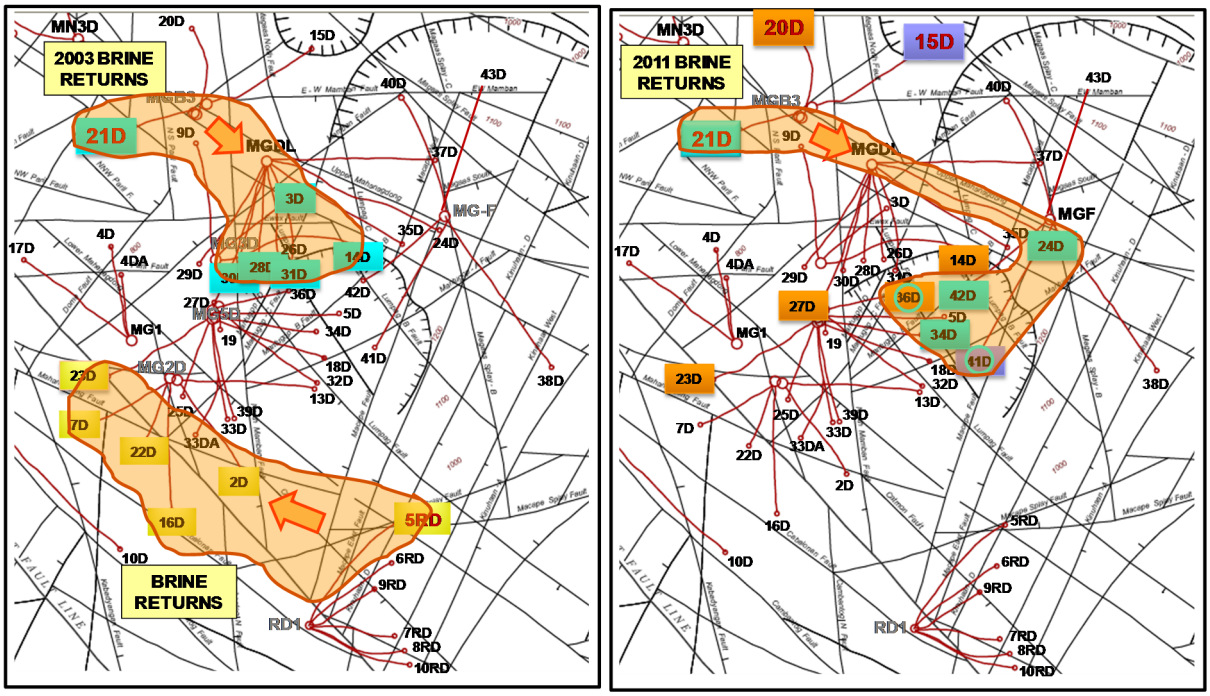

FIGURE 25: Comparison of the extent of brine returns, based on 2003 and 2011 tracer tests; Extent of brine returns in the 2003 tracer test (left); Extent of brine returns in the 2011 tracer test (right)

In the 2003 tracer test, brine returns from well MG-21D yielded a positive response in 5 wells (MG-3D, MG-28D, MG-30D, MG-31D, and MG-14D) in the central production area. Comparing this with the 2011 tracer test, the 5 positive wells in the 2003 tracer test no longer showed a positive tracer response from well MG-21D. Instead, 5 wells in the eastern part of the field showed a positive response. Only one of these wells (MG-24D) was online when the 2003 tracer test was conducted while the 4 remaining wells (MG-34D, MG-36D, MG-41D, and MG-42D) are relatively new wells which were drilled after 2004. It appears from these results that brine returns from well MG-21D shifted from affecting the central production area to further east of the field. The probable underlying reason for this shift of hydrologic flow to the east will be expounded in subsequent discussions.

Although the comparison shows that there only seems to be a shift of well MG-21D brine flow to the east, the total mass recovery and the tracer return profiles of the affected wells between the 2003 and

2011 tracer tests differ significantly. In the 2003 tracer test, the total tracer mass recovery from the 5 1,5-NDS tracer affected wells was 3.76% or 23 kg out of 600 kg of tracer injected. However, in the 2011 tracer test, a mere 0.46% of tracer was recovered from the 5 affected wells, or 2.4 kg out of 550 kg of tracer injected. Tracer return profiles of the affected wells in the 2003 tracer test exhibit the characteristic bell-shaped curve tracer response, allowing for inverse modelling of the 5 wells to estimate the flow-channel properties. In the 2011 tracer test, only well MG-36D showed a definitive tracer response; the other 4 tracer-positive wells showed very sparse data points and incomplete tracer return profiles, which do not allow for reliable inverse modelling. Cooling predictions also significantly differ: the 2003 tracer test, which had higher tracer recoveries, indicated that a maximum of 2.5°C temperature decline would occur in the next 4-7 years in the tracer-positive wells. But according to the 2011 tracer test, only a maximum of ~0.05°C temperature decline is predicted in 20 years. Taken altogether, these differences suggest that unlike the conditions of the 2003 tracer test, the effect of brine returns from the northern injection sink under the conditions of the 2011 tracer test is deemed to have no significant effect on the production sector.

Figure 26 shows the apparent extent of groundwater inflow to the production sector during the 2003 and 2011 tracer tests. While only 6 wells were affected in the 2003 tracer test, 7 additional wells were affected in the 2011 tracer test, for a total of 13 affected production wells. The 2011 tracer test indicates that the groundwater inflow has further extended to the southern and eastern parts of the field. Total tracer recovery has also increased from the 2003 recovery of 19% (114 kg out of 600 kg injected) to a 23.4% recovery (128.7 kg out of 550 kg) in 2011. The speed of groundwater inflow towards the production sector also appears to be a lot faster compared to the 2003 tracer test, as evidenced by the number of days to the first tracer breakthrough (Figure 27).

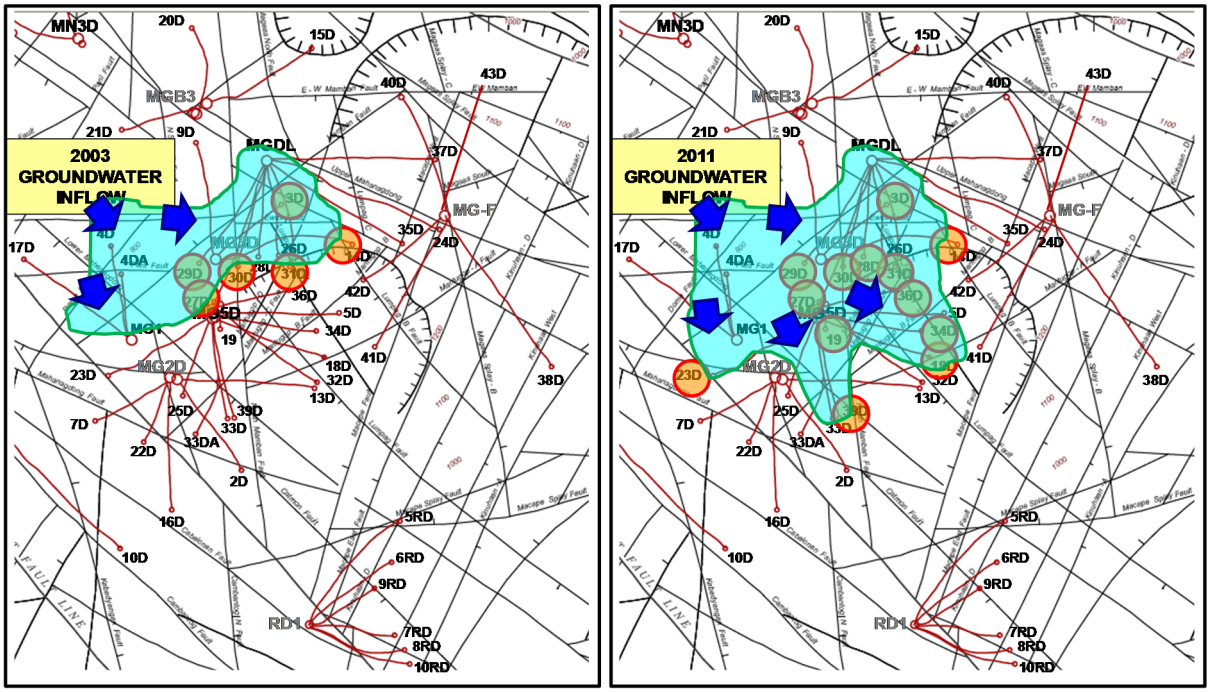

FIGURE 26: Comparison of the extent of groundwater inflow, based on 2003 and 2011 tracer tests; Extent of groundwater inflow in the 2003 tracer test (left); Extent of groundwater inflow in the 2011 tracer test (right)

While the 2003 tracer test indicated that the groundwater inflow from the west would have no significant cooling effect on the 6 tracer-positive wells at that time, results of the 2011 tracer test indicate that this is no longer the case (if indeed it was the case). Encroachment of groundwater from the west towards the production sector appears to be the dominant reservoir process which is causing a deleterious effect in the steam supply of Mahanagdong. It has already been shown that this inflow encroaches much faster

than at the time of the 2003 tracer test, and is predicted to affect more wells in the production sector. Results of the groundwater inflow modelling in Section 5.4 also predict that if this encroachment is left unmitigated, reservoir temperature will continue to decline, posing a serious threat to the sustainability of utilizing the geothermal field.

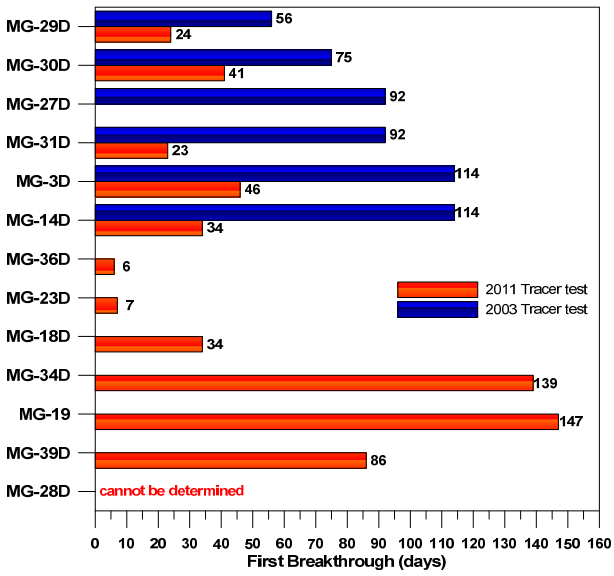

FIGURE 27: Number of days to the first tracer breakthrough for the groundwater inflow-affected wells

5.6 Resource management interventions

The importance of formulating and implementing sound resource management interventions cannot be overstated. These resource management interventions should not only be theoretically reasonable, but should also be implemented in the swiftest way possible so as to mitigate the alarming effects of groundwater encroachment on the production sector. Management interventions, with regard to reinjection strategies, preventing, or reducing groundwater encroachment, long-term field development, and developing a more detailed 3D numerical model, are hereby presented.

5.6.1 Proposed reinjection strategies

Reinjection strategies in the northern injection sink must be geared towards providing the optimum pressure support in the production sector. It should be pointed out that the primary cause for faster encroachment of groundwater is the worsening pressure drawdown caused by massive mass extraction, especially in the central production area where wells are densely-spaced. The only way to counteract this massive pressure drawdown is by optimum reinjection in the northern injection sink.

Results of the thermal interference modelling for well MG-21D, discussed in Section 5.3.1, indicate that even with a 150 kg/s reinjection load, the expected degree of cooling in well MG-36D will only be about 0.8°C. Since well MG-21D has a maximum measured reinjection capacity of 137 kg/s (February 2009 tracer flow test), thermal interference modelling suggests that with the current reservoir conditions where groundwater encroachment into the production sector has already occurred, reinjection at maximum well capacity would have no appreciable effect on the production sector. It is, therefore, recommended to further increase the reinjection load in well MG-21D from the current average of 46 kg/s to a much higher load that could be accepted by the well.

This recommendation of maximum reinjection in well MG-21D goes against the conventional resource management strategy implemented after the 2003 tracer test in which the load for well MG-21D was optimized at 40-60 kg/s. The rationale behind this MG-21D load optimization strategy was to strike a balance between providing pressure support, on one hand, and preventing significant temperature decline on the other. However, results of the current tracer study indicate that this strategy has not been effective. If it was effective, then it would have successfully prevented further encroachment of the groundwater on the eastern part of the field. Also, as clearly shown in Figure 28, groundwater inflow and the change in the production pattern seem to have redirected the flow of brine from well MG-21D since the 2003 tracer test. It must be noted that since 2003, there has been a decrease in mass extraction in the central production area due to wellbore blockages and shutting of non-commercial wells (MG-26D, MG-33D, MG-1), as well as intermittent use of wells MG-27D and MG-29D which are prone to collapse. However, additional mass extraction in the N-NE region offsets this decrease in mass extraction, such that the 2003 and 2011 extraction rates are comparable at 1000-1100 kg/s. Brine flow

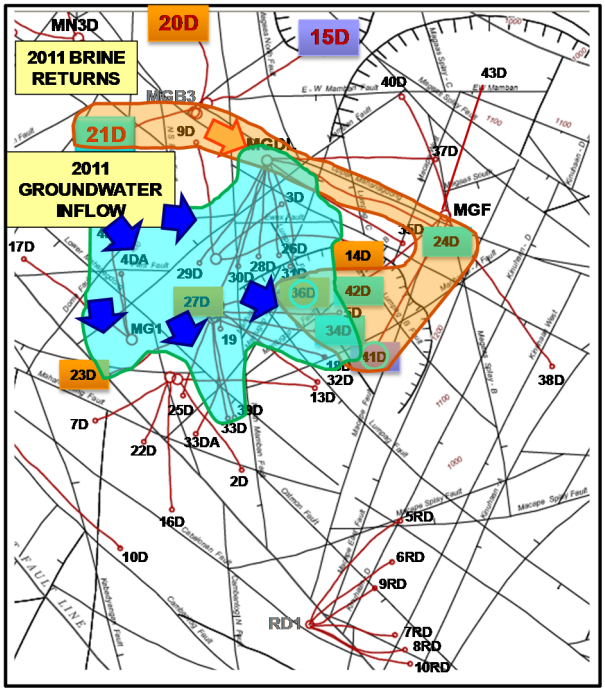

FIGURE 28: Extent of groundwater inflow and brine returns based on 2011 tracer test

from well MG-21D used to preferentially flow towards the central production area in 2003, but in 2011 the brine appears to be flowing instead to the eastern part, as a result of the faster and more voluminous inflow of groundwater. Maintaining the MG-21D load at 40-60 kg/s would only maintain the current rate of groundwater encroachment.

But if the reinjection load of well MG-21D will be maximized, say to more than a 100 kg/s (depending on the well capacity) and sufficient pressure support is to be achieved so as to prevent groundwater from encroaching on the production sector, then the question is whether it would not just cause a similar deleterious effect as the groundwater inflow? This is not quite the case. It should be noted that although groundwater downflow in well MG-4DA has a measured temperature of about 165-170°C, well MG-4DA is located very near the production sector and, therefore, provides less time for reheating fluids. Reservoir temperatures near well MG-4DA are also much lower compared to the reservoir temperatures in the northern injection sink. In contrast, 165-170°C brine injected into well MG-21D could be reheated further as it travels towards the production sector, owing to the much longer distance and higher reservoir temperatures in the area. Another compelling reason for why maximum reinjection in well MG-21D would not have a similar effect as the groundwater inflow is the presence of the general groundwater inflow modelled in Section 5.4. This general groundwater inflow was inferred to be the major culprit for the rapid temperature decline in the 1,6-NDS tracer-positive wells, not the fluids from well MG-4DA. If maximum reinjection in well MG-21D is implemented, this general groundwater inflow would be weakened and, coupled with pre-emptive groundwater encroachment strategy, might just be the solution in combating the groundwater encroachment. This pre-emptive groundwater encroachment strategy will be discussed further in the next section.

While implementing maximum reinjection in well MG-21D (greater than 60 kg/s) is hoped to provide further pressure support in preventing the worsening groundwater encroachment, this strategy still needs to be monitored by conducting another tracer test after this strategy is implemented. Conducting another tracer test will verify the effectiveness of the recommended strategy and, at the same time, will provide an updated scenario of the hydrological flow of peripheral fluids. The time as to when this next tracer test should be conducted can be simulated, based on the implemented reinjection load of well MG-21D. The routine physical and chemical monitoring of the production wells will also provide vital indications about changes in reservoir processes, so both simulation and physicochemical parameters must be considered in determining the best time for conducting another tracer test.

Maximizing the reinjection load of well MG-21D was deemed to be a priority reinjection strategy as MG-21D is the nearest reinjection well to the production sector, compared to the two other reinjection wells MG-20D and MG-15D. However, if well MG-21D is already operating at maximum capacity, then the next best reinjection strategy – if more hot brine is to be disposed of – is to operate the two remaining northern reinjection wells at their full capacity.

It should be stressed at this point that although well MG-4DA has already been shut for more than 5 years, its intermittent use as an "emergency" cold brine reinjection well (to reduce the brine level in the thermal pond) should be stopped at once. The natural downflow of well MG-4DA – which has a much

higher temperature compared to the "emergency cold brine" intermittently reinjected – poses a serious problem in the production sector; injecting additional cold brine at large quantities would further aggravate the problem.

5.6.2 Pre-emptive groundwater encroachment strategy

The principle involved in a pre-emptive groundwater encroachment strategy is simply to prevent the groundwater from encroaching on the production sector by drawing it in and discharging it through sacrificial wells. Sacrificial wells are wells allowed to continuously discharge to the silencers. These wells should be strategically located near the inferred groundwater source so as to effectively draw in the groundwater and reduce the impacts on the production sector.

MG-1, a non-commercial vertical well near well MG-4DA, was discharged as a sacrificial well in October 2009 until November 2010, but was then shut due to problems in cold brine disposal. It was planned to be the first sacrificial well fronting the inferred groundwater source. To date, the well is still shut and is waiting to be discharged again.

MG-26D, another non-commercial well drilled in the central production area, has been used as a sacrificial well in the past but like well MG-1, has also been shut due to problems in brine disposal. Utilization of this well as a sacrificial well has been shown to have improved the performance of nearby well MG-31D. However, since the well has been shut for more than 2 years already, its full benefit as a sacrificial well remains to be seen once the well is re-discharged again as soon as the current brine disposal limitations are addressed.

Another production well in the central production area, MG-27D, has been observed to frequently collapse in the last 2 years. The temperature decline in this well was modelled in Figure 24, and the current evaluation of the physical and chemical parameters indicates that the well is affected by groundwater inflow. If this difficulty in attaining commercial wellhead pressure continues to the point of rendering the well unfit for production, MG-27D would be a good candidate for a sacrificial well as it is located closer to the inferred groundwater source and could effectively front the inflow, preventing it from encroaching on other production wells.

The full merit of utilizing sacrificial wells still remains to be seen. Currently, these sacrificial wells cannot be discharged due to challenges in brine disposal. These challenges must be addressed first and must be prioritized in order to realize the potential alleviating effect of sacrificial wells.

It is worth mentioning that if utilization of sacrificial wells is proven to be an effective strategy, energy from these wells could be utilized for binary generation. This possibility would especially be worth looking into if additional sacrificial wells were needed in the long-term. However, this poses the question of where to reinject the fluids extracted from the sacrificial wells, in order to cause a minimal effect on the production sector. Disposal of extracted fluids from future sacrificial wells should, therefore, be carefully planned.

5.6.3 Long-term field development strategy

The steam shortfall in Mahanagdong poses a need to drill additional make-up and replacement wells. However, results of the current study reveal that increasing the mass extraction in the groundwater-flooded production area could just worsen the encroachment of groundwater. To resolve this, it is recommended that, instead of drilling new wells in the already drawn down production area, future make-up and replacement wells be targeted instead in the N-NE region of Mahanagdong (near well MG-43D). Recent reservoir re-evaluation conducted by Mondejar et al. (2011) indicated that the N-NE region looks promising as temperatures are greater than 300°C. However, development in this region presents challenges in handling the acidic discharges shown by wells MG-40D and MG-43D. It is,

therefore, imperative to develop this region once the on-going acid inhibition studies show significant promise.

Another long-term development strategy worth looking into is the possibility of drilling wells much deeper than the current production depths. This strategy would aim to tap the deeper feed zones in the production area. Following this course of action would only make sense if there is compelling evidence, based on future studies, that only the shallower feed zones are affected by groundwater encroachment. If this appears to be the case, corroborated by future studies, then it would be reasonable to drill deeper wells and set the production casing shoe at depths where groundwater could no longer penetrate.

5.6.4 3D Numerical modelling

A 3D numerical model of the Greater Tongonan geothermal field was recently developed in collaboration with the University of Auckland in New Zealand. The model covers both the Tongonan geothermal field in the north, and Mahanagdong geothermal field in the south. However, the current numerical model of Mahanagdong is unable to reproduce the effects of groundwater inflow on the production sector. The current numerical model would also not be able to simulate the results of the 2011 tracer test.

As demonstrated in the preceding discussion on the 2011 tracer test results, modelling the encroachment of groundwater inflow on the production sector is of primary importance in coming up with reliable predictions of future reservoir behaviour. Reproducing the tracer test results in the numerical model would also enable a deeper understanding of the reservoir processes. With this in mind, it is recommended to develop a new 3D numerical model specifically for Mahanagdong. Although this recommended model would still cover the Tongonan geothermal field in the north, the model grid for Tongonan would be much coarser as this is not the area of interest. On the other hand, Mahanagdong would have a finer grid – much finer than in the current numerical model – able to simulate the results of the 2011 tracer test and allow for detailed modelling of groundwater inflow.

The merit of developing a new 3D numerical model for Mahanagdong mainly lies in its envisioned ability to reproduce the groundwater inflow and the results of the 2011 tracer test. Accomplishing this would be a powerful tool, not only due to the increased accuracy in predicting various production scenarios. If the recommended 3D numerical model could indeed reproduce the prevailing reservoir process of groundwater encroachment, then it would be able to shed light on the feasibility of drilling additional sacrificial wells targeted towards the inferred groundwater source. The recommended 3D numerical model would be able to simulate the effect of drilling additional sacrificial wells and would, therefore, lessen the financial risks in implementing pre-emptive groundwater encroachment strategies. It must also be mentioned that since developing a 3D numerical model would cost much less than immediately drilling additional sacrificial wells, it would be a more prudent course of action.

6. SUMMARY AND CONCLUSIONS

This paper has presented and discussed the results of a 2011 tracer test, using four types of naphthalene disulfonate tracer, conducted from June 2011 to June 2012 in the Mahanagdong geothermal field, Philippines. Three different types of NDS tracer were injected in three reinjection wells (MG-15D, MG-20D, and MG-21D) in the field's northern injection sink to evaluate the inflow of brine returns. A fourth type of NDS tracer was injected into well MG-4DA in the western part of the field to trace the inflow of groundwater into the production sector.

The 2,6-NDS tracer injected in well MG-15D yielded only one positive response in well MG-41D out of the 26 monitored wells. The 2,7-NDS tracer injected in well MG-20D yielded 4 positive responses in wells MG-14D, MG-23D, MG-27D, and MG-36D. Tracer recovery from wells MG-15D and MG-

20D was very low at 0.05 and 0.35%, respectively. Tracer return profiles were also highly sparse with very few instances of tracer detection. The 1,5-NDS tracer injected in well MG-21D yielded 5 positive responses in wells MG-36D, MG-24D, MG-34D, MG-41D, and MG-42D. Cumulative 1,5-NDS tracer recovery was also very low at only 0.43%. Of all the tracer-positive wells from the three types of tracer injected in the northern injection sink, only the 1,5-NDS tracer-affected well MG-36D had a definitive tracer recovery which allowed for reliable inverse modelling of flow-channel properties. Thermal interference modelling of well MG-36D tracer response indicated that a long-term reinjection of 46 kg/s for 20 years would cause a minimal temperature decline of ~0.12°C. Results also suggested that even at 150 kg/s reinjection load, the expected degree of cooling in well MG-36D would be about 0.4°C. Taken together, these results suggest that under the conditions during the tracer monitoring, reinjection in the northern injection sink would not cause a significant return of reinjected brine as to have any appreciable thermal interference in the production sector.

Tracer recovery monitoring of 1,6-NDS tracer injected in well MG-4DA produced disquieting results as 13 of the 26 monitored wells yielded positive returns with a relatively high percentage of mass recoveries and fast breakthroughs. Of the 13 1,6-NDS tracer-positive wells, tracer return profiles of 9 wells were simulated as the other 4 tracer-positive wells did not provide satisfactory data for inverse modelling. Thermal interference modelling indicated that at the pessimistic scenario of a 10 kg/s downflow rate in well MG-4DA, well MG-36D would have the highest predicted temperature decline of 1.4°C in 20 years. All other wells had negligible temperature decline, based on the model.

The predicted degree of cooling of the 1,6-NDS tracer-positive wells was then compared with the actual cooling observed. Data on measured cooling from 2003 to date indicated that the actual temperature decline of all the affected wells was higher than the predicted temperature decline, even after 20 years. This finding suggested that an even greater inflow of groundwater – greater than the downflow observed in well MG-4DA – exists and must, therefore, be estimated. Groundwater inflow modelling was conducted and results revealed that the rate of groundwater inflow to the production sector was estimated to be around 200-300 kg/s. Calculation of the average groundwater velocity indicated that the groundwater inflow velocity and the velocity of fluids from well MG-4DA were comparable, with calculated velocities of 195 $\pm$ 120 m/month and 292 $\pm$ 95 m/month, respectively. The fact that the calculated velocities of 195 $\pm$ 120 m/month and 292 $\pm$ 95 m/month were within each other´s standard deviations implied that the tracer carried by the downflow in the wells travels with the general groundwater flow as well. This suggested that the downflow observed in well MG-4DA could most likely be just a small part of a much greater groundwater inflow towards the production sector.

While the 2003 tracer test indicated that the groundwater inflow from the west would have no significant cooling effect on the 6 tracer-positive wells at that time, results of the 2011 tracer test indicated that this is no longer the case (if indeed it ever was). Encroachment of groundwater from the west on the production sector appears to be the dominant reservoir process in Mahanagdong, and is now occurring at an even faster rate. Results of the groundwater inflow modelling predicted that if this encroachment was left unmitigated, reservoir temperature would continue to decline, posing a serious threat to the sustainability of the geothermal field. To mitigate the alarming effect of groundwater encroachment on the production sector, resource management interventions must be implemented as soon as possible. Management interventions with regard to reinjection strategies, preventing, or reducing, groundwater encroachment, long-term field development, and developing a more detailed 3D numerical model were presented.

7. RECOMMENDATIONS AND FUTURE WORK

Part of the resource management interventions recommended in this paper was to develop a more detailed 3D numerical model of Mahanagdong in order to simulate the effects of groundwater inflow on the production sector, and simulate as well the results of the tracer test. The author hopes to develop

this model because it would provide valuable and vital insight into managing the reservoir and ensuring its sustainability. Aside from providing a more accurate forecast of different production scenarios, the numerical model would be able to shed light on the feasibility of drilling additional sacrificial wells, precisely aimed at preventing, or reducing, groundwater encroachment. The model would also provide more confidence in future resource management strategies and would, consequently, be a powerful tool in lowering financial risks.

In addition to developing a detailed 3D numerical model, it is recommended to increase the brine reinjection load of well MG-21D from the current load of 40-60 kg/s to more than 60 kg/s, depending on the maximum reinjection capacity of the well. Thermal interference modelling indicated that even a 150 kg/s MG-21D reinjection load would not cause a significant thermal effect, so the increased load could provide more pressure support in the groundwater-flooded production area. After the MG-21D maximum reinjection strategy is implemented, it is recommended to conduct another tracer test to verify the effectiveness of the recommended strategy and simultaneously provide an updated scenario of the hydrological flow of peripheral fluids. If well MG-21D is already operating at maximum capacity, then the next best reinjection strategy – if more hot brine was to be disposed of – is to operate the two remaining northern reinjection wells, MG-20D and MG-15D, at their full capacity. Intermittent use of well MG-4DA as an "emergency" cold brine reinjection well should be stopped at once. Utilization of sacrificial wells MG-1 and MG-26D should be continued in order to realize the potential alleviating effect of sacrificial wells. If utilization of sacrificial wells is proven to be an effective strategy, the possibility of utilizing the energy from sacrificial wells for binary generation should be considered. This possibility would especially be worth looking into if additional sacrificial wells were needed in the long-term. For long-term field development strategy, it is recommended that instead of drilling new wells in the already drawn down production area, future make-up and replacement wells be targeted instead in the N-NE region of Mahanagdong. However, since the N-NE region hosts acidic fluids, it is imperative to develop this region only if on-going acid inhibition studies show significant promise. Another recommended long-term development strategy is the possibility of drilling wells much deeper than the current production depths. If future evidence showed that deeper feed zones could be exploited, deeper drilling should be considered with the production casing shoe set at depths unaffected by groundwater inflow.

ACKNOWLEDGEMENTS

Isaac Newton is credited for saying, "If I have seen further than others, it is by standing upon the shoulders of giants." In the same spirit of humility and gratitude, let me express here my warmest appreciation and gratitude to the giants upon whose shoulders I have been standing…

… to my UNU-GTP family under the dedicated and esteemed staff of Dr. Ingvar Birgir Fridleifsson (Director), Mr. Lúdvík S. Georgsson (Deputy Director), Mr. Ingimar Gudni Haraldsson (Project Manager), Ms. Málfrídur Ómarsdottir (Environmental Scientist), Ms. Thórhildur Ísberg, and Mr. Markus A.G. Wilde. Thank you for making my UNU Fellowship in Iceland a learning-filled, fun, and memorable experience.

… to the management of Energy Development Corporation: President Richard B. Tantoco, and Senior Vice-President of Technical Services Sector, Manuel S. Ogena, thank you for believing in me and for supporting my Fellowship; to the Vice-President of the Resource Management Division, Ka Noel D. Salonga, for encouraging me to look for other universities and institutions that would provide better training in reservoir engineering; to Engr. Edwin H. Alcober, for being the most supportive manager; to Engr. Romeo P. Andrino Jr., for being so patient with me and for being the best boss ever; to my colleagues in the LGBU Resource Evaluation and Sustainability Group, especially to Ate Lorena Daco-ag, Regina Cabahug, and Kenneth Faja, for putting up with my questions and data requests; to Anthony Ciriaco and Selna Ledesma, for providing inputs in numerical modelling. And of course, to Engr.

Erlindo C. Angcoy Jr., whom I deeply look up to and admire, thank you for opening the door for me to be able to study here in UNU-GTP.

… to my family, for all the love and emotional support. To my mom and my three siblings, you always inspire me to give my best in everything I do; to Ciara Christianne Lim, just because I want to mention your name here.

… and, finally, to my supervisor, Dr. Gudni Axelsson. Thank you Gudni for all the guidance while doing the project, for reminding me to rest enough and to learn to enjoy the journey, for putting up with my silly questions, and for inspiring me to be a better reservoir engineer. Someday, I will be better than you… someday.

REFERENCES

Angcoy Jr., E.C., 2011: *Mahanagdong geochemistry – an alternative data analysis.* EDC, Pasig City, internal report (unpublished).

Angcoy Jr., E.C., Alcober, E.H., Sta. Ana., F.X.M., Cabel Jr., A.C., Bayrante, L.F., Malate, R.C.M., and Ogena, M.S., 2008: Conquering the challenges in geothermal utilization - the EDC experience. *Presented at "30th Anniversary Workshop of the United Nations University Geothermal Training Programme" organized by UNU-GTP, Reykjavik, Iceland*, 8 pp.

Arason, Th., 1993a: Program TRMASS. In: Arason, Th., Björnsson, G., Axelsson, G., Bjarnason, J.Ö., and Helgason, P., 2004: *ICEBOX – Geothermal reservoir engineering software for Windows. A user's manual.* ÍSOR, Reykjavík, report ISOR-2004/014, 80 pp.

Arason, Th., 1993b: Program TRINV. In: Arason, Th., Björnsson, G., Axelsson, G., Bjarnason, J.Ö., and Helgason, P., 2004: *ICEBOX – Geothermal reservoir engineering software for Windows. A user's manual.* ÍSOR, Reykjavík, report ISOR-2004/014, 80 pp.

Arason, Th., Björnsson, G., Axelsson, G., Bjarnason, J.Ö., and Helgason, P., 2004: *ICEBOX – Geothermal reservoir engineering software for Windows. A user's manual.* ÍSOR, Reykjavík, report 2004/014, 80 pp.

Austria, R.O., and Villareal, M.Z., 2011: *Preliminary volcano-tectonic study of Mahanagdong sector, Tongonan geothermal project.* EDC, Pasig City, internal report (unpublished).

Axelsson, G., 2012: Role and management of geothermal reinjection. *Presented at "Short Course on Geothermal Development and Geothermal Wells", organized by UNU-GTP and La Geo, Santa Tecla, El Salvador,* 21pp.

Axelsson, G., Björnsson, G., and Arason, Th., 1994: Program TRCOOL. In: Arason, Th., Björnsson, G., Axelsson, G., Bjarnason, J.Ö., and Helgason, P., 2004: *ICEBOX – Geothermal reservoir engineering software for Windows. A user's manual.* ÍSOR, Reykjavík, report ISOR-2004/014, 80 pp.

Axelsson, G., Björnsson, G., and Montalvo, F., 2005: Quantitative interpretation of tracer test data. *Proceedings of the World Geothermal Congress 2005, Antalya, Turkey,* 12 pp.

Axelsson, G., Flóvenz, O.G., Hauksdóttir, S., Hjartarson, A., and Liu, J., 2001: Analysis of tracer test data, and injection-induced cooling, in the Laugaland geothermal field, N-Iceland. *Geothermics, 30,* 697-725.

Belas-Dacillo, K.A., Alcober, E.H., Andrino, R.P., Angcoy Jr., E.C., Arones, R.G., Baltazar Jr., A.D., Daco-ag, L.C., Mondejar, G.C., Sabenicio, M.C., 2010: *Providing solutions to the new challenges in the Mahanagdong resource*. EDC, Pasig City, internal report (unpublished).

Caranto, J.A, and Jara, M.P., 2006: Factors controlling reservoir permeability at the Leyte geothermal production field, Tongonan, Philippines. *Proceedings of the 27th PNOC-EDC Geothermal Conference*, *Makati City, Philippines*, 107-112.

Daco-ag, L.C., 2011: *Mahanagdong resource assessment geochemistry update.* EDC, Pasig City, internal report (unpublished).

Delfin, F.G., Dacillo, D.B., and Marcelo, E.A., 2001: Analysis and interpretation of ^{125}I tracer test results, Mahanagdong geothermal reservoir, Leyte, Philippines. *Presented at "IAEA RAS/8/092 and INT/0/060 Coordination Meeting on Isotopic and Geochemical Techniques in Geothermal Exploration and Reservoir Management", Makati City and Cebu City,* 8 pp.

Herras, E.B., and Parilla Jr., E.V., 1995: *Result of the MG-4DA sodium fluorescein tracer test*. EDC, Pasig City, internal report (unpublished).

Herras, E.B., Siega, F.L., and Magdadaro, M.C., 2005: Naphthalene disulfonate tracer test data in the Mahanagdong geothermal field, Leyte, Philippines. *Proceedings of the World Geothermal Congress 2005, Antalya, Turkey*, 7 pp.

Molina, P.O., Tanaka, T., Itoi, R., Siega, F.L., and Ogena, M.S., 2005: Analysis and interpretation of naphthalene disulfonate tracer tests at the Mahanagdong geothermal field, Philippines. *Proceedings of the World Geothermal Congress 2005, Antalya, Turkey*, 9 pp.

Mondejar, G.C., Andrino, R.P., Austria, J.J.C., and Ciriaco, A.E., 2011: *Mahanagdong geothermal resource reservoir update.* EDC, Pasig City, internal report (unpublished).

Olivar, R.O., 2011: *Geophysical review of Mahanagdong geothermal field.* EDC, Pasig City, internal report (unpublished).

Pioquinto, W.C., 2011: *'Quo vadis' in Mahanagdong - re-examining the geo-structural framework of the Mahanagdong geothermal field.* EDC, Pasig City, internal report (unpublished).

Salonga, N.D., Dacillo, D.B., and Siega, F.L., 2004: Providing solutions to the rapid changes induced by stressed production in Mahanagdong geothermal field, Philippines. *Geothermics, 33*, 181-212.

Sta. Ana., F.X.M., Hingoyon-Siega, C.S., and Andrino, R.P., 2002: Mahanagdong geothermal sector, Greater Tongonan geothermal field, Philippines: reservoir evaluation and modelling update. *Proceedings of the 27th Workshop on Geothermal Reservoir Engineering, Stanford University, Stanford, CA*, 7 pp.

APPENDIX I: Mass recovery and time of tracer breakthrough for wells with only one instant of tracer recovery

Monitored well	% Tracer recovery	Time of tracer breakthrough (days)	Tracer concentration (ppb)
2,6-NDS (MG-15D) tracer			
MG-16D	0.03	58	1.03
MG-23D	0.07	268	0.67
MG-27D	0	1	0.23
MG-31D	0.23	261	1.07
MG-34D	0.03	227	0.94
MG-36D	0.04	247	0.50
2,7-NDS (MG-20D) tracer			
MG-3D	0.14	24	13
MG-18D	0	1	0.62
MG-29D	0	1	0.65
MG-31D	0	1	0.66
MG-43D	0.01	34	0.55
1,5-NDS (MG-21D) tracer			
MG-2D	0.01	24	0.57
MG-18D	0.01	17	0.70
MG-27D	0	1	1.05
MG-30D	0.15	228	1.59
MG-31D	0.04	96	0.51
MG-35D	0.01	206	0.56
1,6-NDS (MG-4DA) tracer			
MG-7D	0.01	23.2	0.55
MG-13D	0	0.2	0.78
MG-24D	0	10.0	0.85
MG-32D	0.01	205.2	0.62
MG-35D	0.01	188.2	0.52
MG-37D	0	3.2	0.50
MG-41D	0	9.2	0.53

APPENDIX II: Results of the thermal interference modelling for the 9 1,6-NDS tracer-positive wells

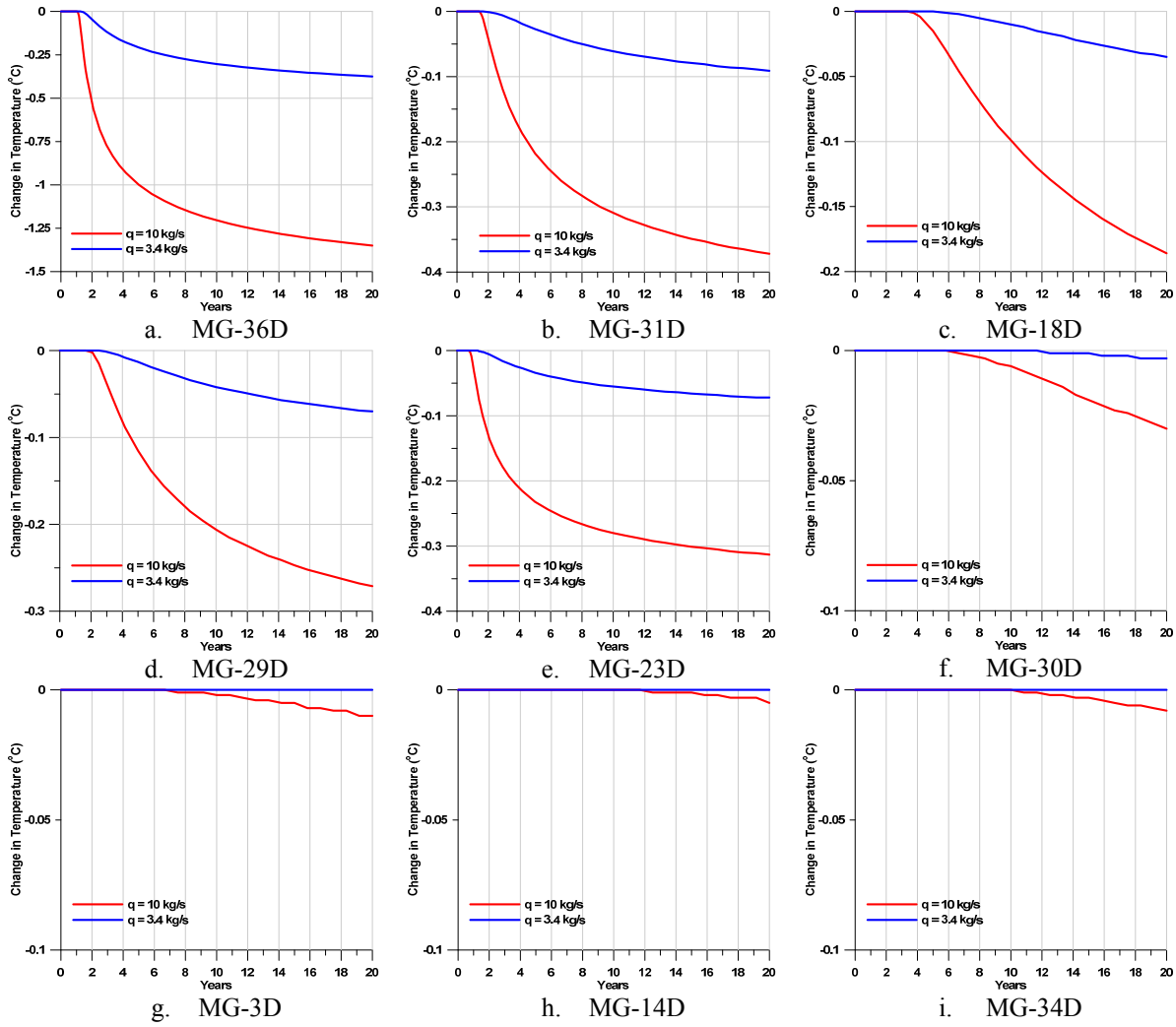

a. MG-36D b. MG-31D c. MG-18D

d. MG-29D e. MG-23D f. MG-30D

g. MG-3D h. MG-14D i. MG-34D